Supporting Information

Effect of Fe(III)-based MOFs on catalytic efficiency of Tandem cyclooxidative reaction between 2-aminobenzamide and alcohols

Minh-Huy Dinh Dang[‡,a,b], Trang Thi Minh Nguyen[‡,a,b], Linh Ho Thuy Nguyen[a,b,] Trang Thi Thu Nguyen[a,b], Thang Bach Phan[a,b], Phuong Hoang Tran[b,c], Tan Le Hoang Doan[a,b*]

[‡]These authors contributed equally to this work.

[a]Center for Innovative Materials and Architectures (INOMAR), Ho Chi Minh City 721337 (Viet Nam)

[b]Vietnam National University-Ho Chi Minh City, Ho Chi Minh City 721337 (Viet Nam)

[c]Department of Organic Chemistry, Faculty of Chemistry, University of Science, Ho Chi Minh City 721337 (Viet Nam)

Email: dlhtan@inomar.edu.vn

Table of Contents

Section 1: Materials and General Methods

Chemicals used in this work. 1,3,5-triphenylbenzene (97% purity),iron (III) chloride hexahydrate,terephthalic acid (98% purity)were obtained from Aldrich Chemical Co.hydrofluoric acid, hydrochloric acid, ethanol (99.5 % purity), methanol (99,8 % purity), sodium hydroxide (97% purity) and sodium sulfate (97% purity) were purchased from Fisher Scientific. 2,6-naphthalenedicarboxylic acid (98% purity), biphenyl-4,4′-dicarboxylic acid (99% purity) were purchased from TCI America.3-nitrobenzoic acid (99 % purity), d-glucose (97% purity), ethyl acetate (anhydrous, purity ≥ 99%), *n*-hexane (anhydrous, purity ≥ 99.5%), Silica gel 230–400 mesh for flash chromatography, TLC plates (silica gel 60 F254)were purchased from Merck Millipore Co.1,4-dioxane (99.9% extra dry grade), 1-butanol (purity ≥ 99%),1-phenylethanol (purity ≥ 98%), 2-aminobenzamide (purity ≥ 98%), 2-propanol (purity ≥ 99%), 4-nitrobenzoic acid (99% purity), 4-methylbenzyl alcohol (purity ≥ 98%), 4-methoxybenzyl alcoShol (purity ≥ 98%),aluminum chloride (anhydrous), acetic acid (99.5% purity), acetone (99.8% extra dry grade), Acetyl chloride (99.5 % purity), benzyl alcohol (purity ≥ 98%),cyclohexanol (purity ≥ 99%), cycloheptanol (purity ≥ 97%), cyclooctanol (purity ≥ 97%), dichloromethane (99.8% extra dry grade), furfuryl alcohol (purity ≥ 98%),iron (III) nitrate nonahydrate (98% purity), *N,N*-dimethylformamide (DMF; 99.8% extra dry grade)were purchased from Acros Organics. NMR solvents: Deuterated solvents D_2O, NaOD/D_2O 40 wt%, and dimethyl sulfoxide-d_6 (DMSO-d_6; 99.9% purity) were purchased from Cambridge Isotope Laboratories. Water used in this work was double distilled and filtered through amillipore membrane.

Analytical techniques. Powder X-ray diffraction data for refinement was collected on a Bruker D8 Advance employing Ni filtered Cu Kα (λ = 1.54059 Å) radiation (Section 3). A liquid N_2 bath was used for measurements at 77 K. Helium was used as estimation of dead space. Ultrahigh-purity-grade N_2 and He (99.999% purity) were used throughout adsorption experiments. Thermogravimetric analysis (TGA) curves were recorded on a TA Q500 thermal analysis system under airflow (Section 4).The air used has a purity of 99.99%. The chemicals were measured by using Sartorius balance.Low-pressure N_2 adsorption measurements were carried out on a Micromeritics 3Flex surface characterization analyzer (Section 5). The reactions were conducted on a CEM Discover SP microwave system. The products were centrifuged by Mikro 200 machine and analyzed by Agilent GC-MS system or thin-layer chromatography

(TCL) performed on F-254 silica gel coated aluminum plates from Merck (Section 6). Column chromatography was performed on silica gel 60, 0.04−0.06 mm (230–400 mesh). Melting points were recorded with a Buchi B-545 melting point Apparatus. Fourier transform infrared (FT-IR) spectra were measured on a Bruker E400 FT-IR spectrometer (Section 7 and 8). Nuclear magnetic resonance (^{1}H and ^{13}C NMR) spectra were acquired on a Bruker advance II 500 MHz NMR spectrometer (Section 7 and 8). Chemical shifts were quoted in parts per million (ppm) and referenced to the appropriate solvent peak. Gas chromatography-mass spectrometry (GC-MS) measurements were carried out on an Agilent GC System 7890 equipped with a mass selective detector (Agilent 5973N) and a capillary DB-5MS column (30 m × 250 µm × 0.25 µm)(Section 7).

Section 2: Synthesis of MOF-907, MOF-908, MOF-909, PCN-280, PCN-285, MIL-126, MIL-88B, MIL-100, MIL-101

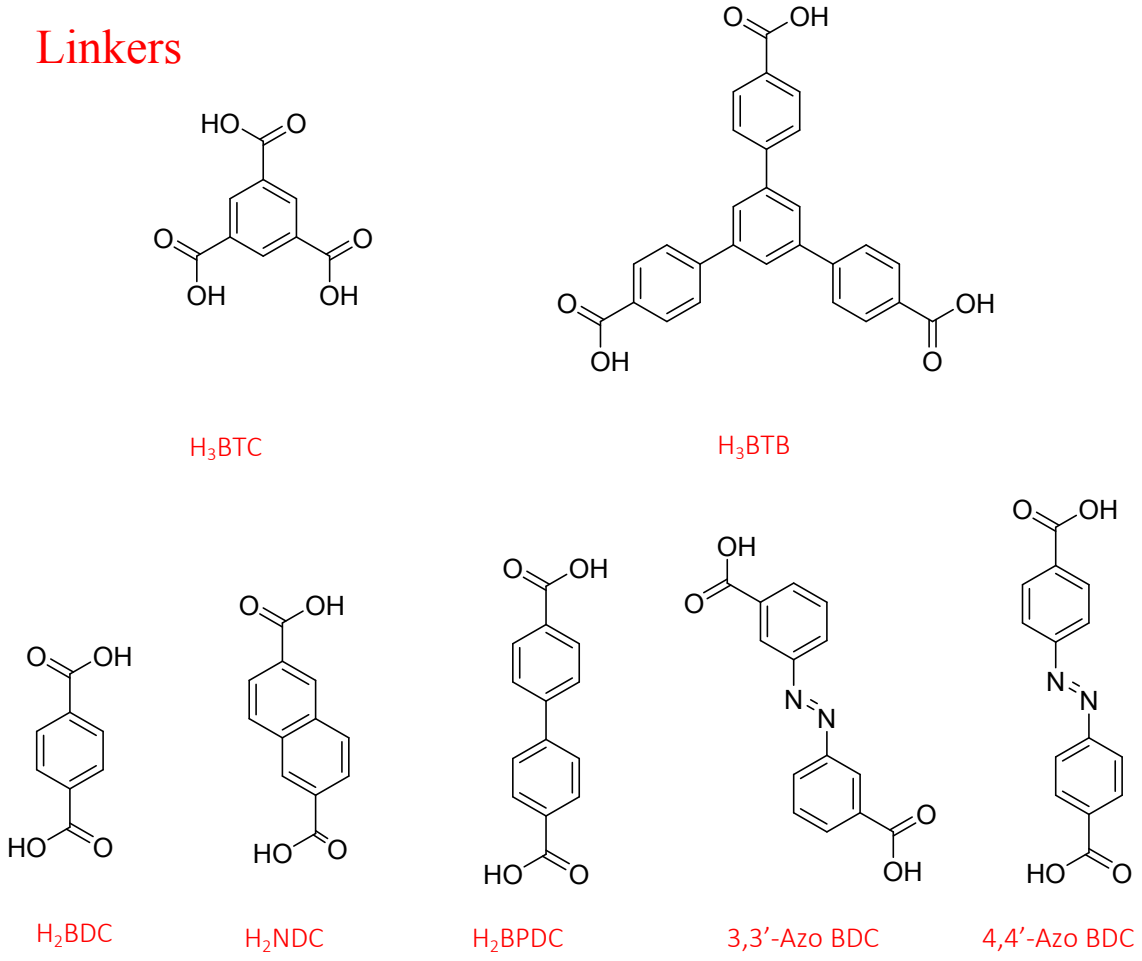

Figure S1. Linkers have been used for the synthesis of Fe-MOFs. Triangular linkers (**Benzene-1,3,5-tricarboxylic acid (H_3BTC),** 4,4′,4”-benzene-1,3,5-triyl-tris(benzoic acid) (H3BTB)) and linear linkers (**Benzene-1,4-dicarboxylic acid linker** (H_2BDC), and 2,6-naphthalenedicarboxylic acid (H_2NDC), 4,4’-biphenyldicarboxylic acid(H2BPDC), 3,3’-azobenzene dicarboxylic acid (3,3’-AzoBDC), 4,4’-azobenzene dicarboxylic acid (4,4’-AzoBDC)).

1,3,5-tris(4-carboxyphenyl)benzene (H_3BTB),azobenzene-3,3’-dicarboxylic acid (3,3’-azoBDC) and azobenzene-4,4’-dicarboxylic acid (4,4‘-azoBDC) were synthesized following the reported procedure.[1-3]

Synthesis of MOF-907:

MOF-907 was synthesized according to a literature procedure.[4]

A mixture of $Fe(NO_3)_3{\cdot}9H_2O$ (0.600 g, 1.5 mmol), 1,3,5-tris(4-carboxyphenyl) benzene (H_3BTB) (0.360 g, 0.81 mmol), and 2,6-Naphthalenedicarboxylic acid (H_2NDC) (0.300 g,1.38 mmol) in *N*,*N*-dimethylformamide (DMF) (120 mL) was added to a 200-mL glass bottle. The procedure was followed by the addition of 6 mL of acetic acid. The mixture was then sonicated for 1 min and isothermally heated at 120 °C for 24 h. The orange powder was cooled down to room temperature and the solid product is washed with DMF (3× 10 mL, each day) for 3 days. After that, the sample was exchanged solvent by acetone (3 × 10 mL, each day) for 3 days. Finally, the sample was activated by heating at 100 °C under low pressure for 24 h leading to obtain109 mg of activated MOF(22.95% yield based on $Fe(NO_3)_3{\cdot}9H_2O$).

Synthesis of MOF-908:

MOF-908 was synthesized according to a literature procedure.[5]

A mixture of $Fe(NO_3)_3{\cdot}9H_2O$ (0.03686g, 0.0912mmol), 1,3,5-tris(4-carboxyphenyl) benzene (H_3BTB) (0.020 g, 0.046 mmol), 4,4’-biphenyldicarboxylic (H_2BPDC) (0.0055 g, 0.023 mmol), and 3,3’-azobenzene dicarboxylic acid (3,3’-AzoBDC) (0.00681 g, 0.025 mmol) was dissolved in a mixture of *N*,*N*-dimethylformamide (DMF, 3.5 mL), 0.5 mL of methanol and 0.2 mL of acetic acid in a 8-mL glass vial. The reaction solution was then heated at 120 °C in an isothermal oven for 24 h to obtain orange shaped crystals. The crystals were thoroughly washed with DMF (3× 10 mL) per day for three days total. After that, the solid was then immersed in acetone (3×

10 mL) per day over a total of three days. The solventexchanged sample was activated under vacuum at ambient temperature for 24 h, followed by heating at 100 C °C under vacuum for 24 h, obtained 14mg of activated MOF (40.64 % yield based on $Fe(NO_3)_3{\cdot}9H_2O$).

Synthesis of MOF-909:

MOF-909 was synthesized according to a literature procedure.[5]

$Fe(NO_3)_3{\cdot}9H_2O$ (0.03686 g, 0.0912 mmol), 1,3,5-tris(4-carboxyphenyl) benzene (H_3BTB) (0.020 g, 0.046 mmol), and 3,3'-azobenzene dicarboxylic acid (3,3'-AzoBDC) (0.01362 g, 0.050 mmol) were added in the mixed of 3.5 mLDMF,0.5mL methanoland 0.2 mLacetic acid . This mixture was then sonicated for 1 min and introduced to an 8-mL glass vial. The solution was heated at 120 °C in an isothermal oven for 24 h. The reaction was then cooled down to room temperature and the solid product is washed with DMF (5 × 3 mL, each day) for 3 days and afterward, the MOF material was exchanged by acetone for 3 days (5 × 3 mL, each day).Finally, The solvent exchanged sample was activated under vacuum at ambient temperature for 24 h, followed by heating at 100 °C under vacuum for an additional 24 h, obtained 9.0mg of activated MOF (27 % yield based on $Fe(NO_3)_3{\cdot}9H_2O$.

Synthesis of PCN-280:

The synthetic procedure of PCN-280 was slightly modified comparing to the original report.[6]

$Fe(NO_3)_3{\cdot}9H_2O$ (0.03686 g, 0.0912 mmol), 1,3,5-tris(4-carboxyphenyl) benzene (H_3BTB) (0.020 g, 0.046 mmol), and biphenyl-4,4′-dicarboxylic acid (H_2BPDC) (0.011 g, 0.046 mmol) were added in the mixture of *N*,*N*-dimethylformamide (DMF, 3.5 mL), methanol (0.5 mL) and acetic acid (0.2 mL) and then introduced to an 8-mL glass vial. The mixture was sonicated for 1 min to obtain a clear solution. Subsequently, this solution was placed in an isothermal oven at 120 °C for 24 h to obtain the orange shaped crystals of PCN-280. The solid was washed with DMF (5 × 3 mL, each day) for 3 days. After that, the sample was exchanged solvent by acetone for 3 days (5 × 3 mL, each day). The solvent-exchanged sample was activated by heating at 80 °C under low pressure for 24 h producing 14mg of activated MOF (53% yield based on $Fe(NO_3)_3{\cdot}9H_2O$).

Synthesis of PCN-285:

The synthetic procedure of PCN-285 was slightly modified comparing to the original report.[6]

A solid mixture of $Fe(NO_3)_3{\cdot}9H_2O$, 1,3,5-tris(4-carboxyphenyl) benzene (H_3BTB) (0.020 g, 0.046 mmol), and 4,4'-azobenzene dicarboxylic acid (4,4'-AzoBDC) (0.01362 g, 0.050 mmol) was dissolved in *N*,*N*-dimethylformamide (DMF, 3.5 mL) in a 8-mL glass vial. The procedure was followed by the addition of 6 mL of acetic acid. The mixture was then sonicated for 1 min and isothermally heated at 120 °C for 24 h. The orange crystalline product was collected after cooling down to room temperature and washed with DMF (5 × 3 mL, each day) for 3 days, exchanged with acetone (5 × 3 mL, each day) for 3 days. The solvent-exchanged sample was activated by heating at 80 °C under low pressure for 24 h producing 6mg of activated MOF (36% yield based on $Fe(NO_3)_3{\cdot}9H_2O$).

Synthesis of MIL-126, MIL-88B, MIL-100 (Fe), MIL-101 (Fe)

Mil-126,Mil-88B,Mil-100 (Fe), MIL-101 (Fe) were synthesized according to the reported procedure.[7-10]

Section 3: Powder X-ray Diffraction Patterns of Fe-MOF Materials

PXRD data was collected using a Bruker D8 Advance diffractometer in reflectance Bragg-Brentano geometry employing Ni filtered Cu Kα focused radiation (1.54059 Å, 1.54439 Å) at 1600 W (40 kV, 40 mA) power. The PXRD instrument is equipped with a LynxEye detector. The best counting statistics were achieved by collecting samples using a 0.02° 2θ step scan from 3 – 30° with exposure time of 0.25 s per step. The measurement was performed at room temperature and atmospheric pressure.

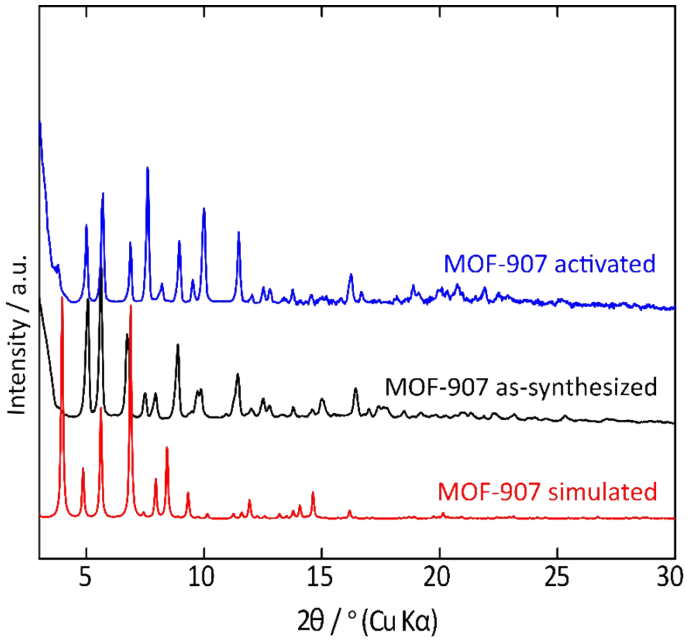

Figure S2.PXRD of simulated MOF-907compared to as-synthesized and activated PXRD patterns

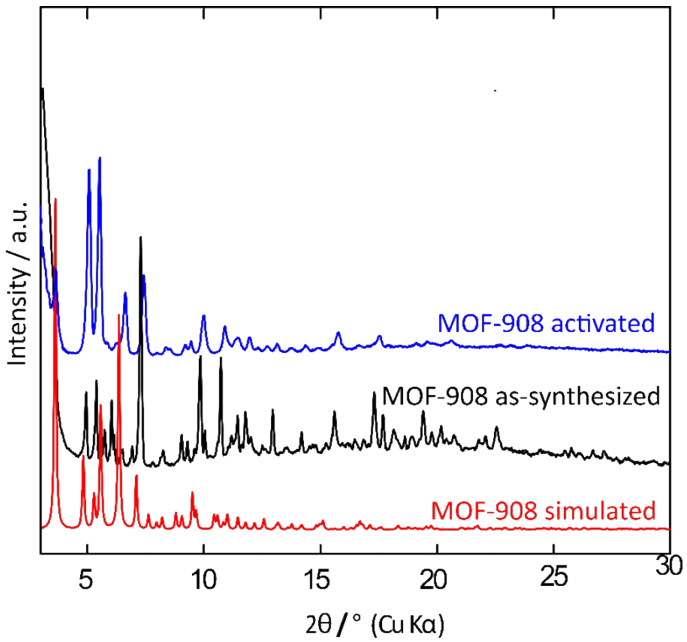

Figure S3. PXRD of simulated MOF-908 compared to as-synthesized and activated PXRD patterns.

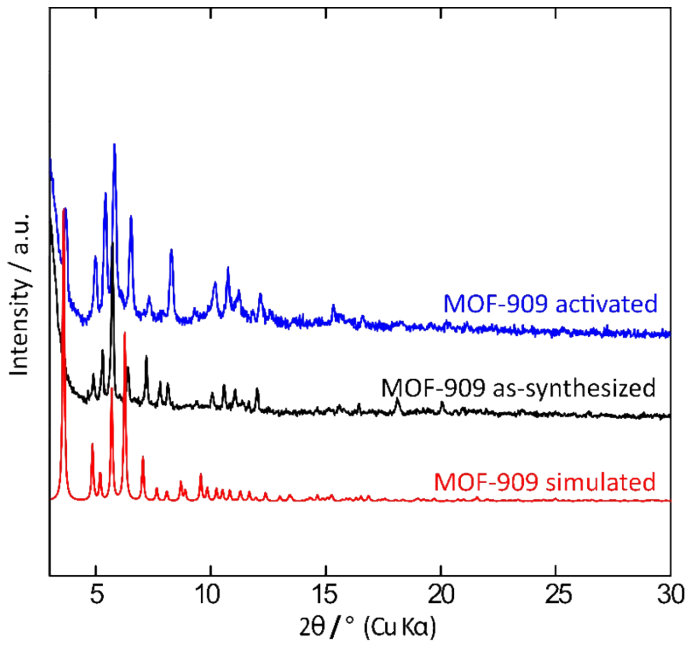

Figure S4. PXRD of simulated MOF-909 compared to as-synthesized and activated PXRD patterns.

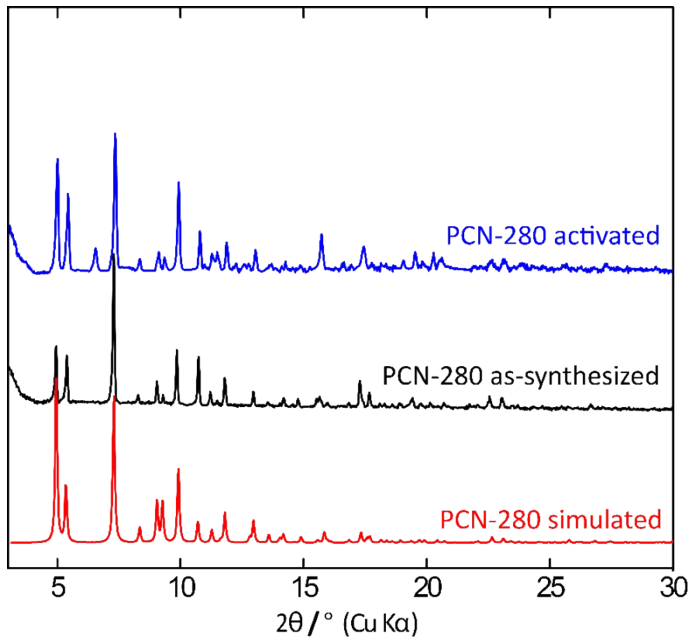

Figure S5. PXRD of simulated PCN-280 compared to as-synthesized and activated PXRD patterns

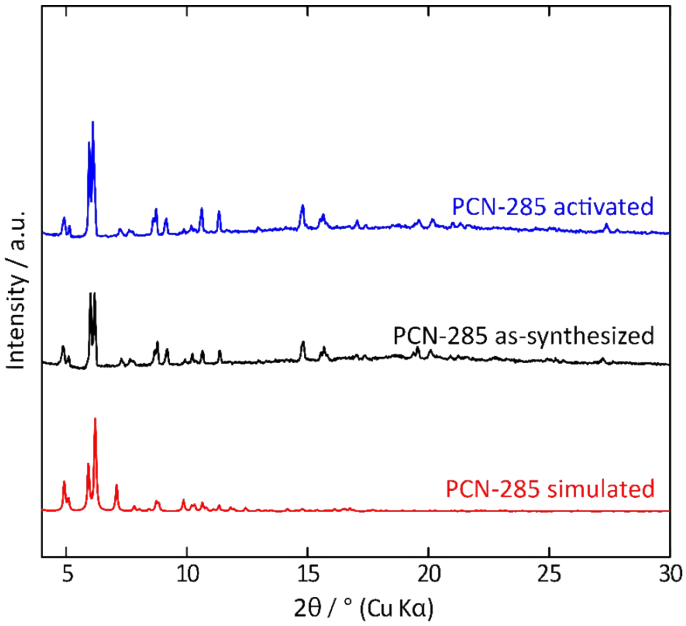

Figure S6. PXRD of simulatedPCN-285 compared to as-synthesized and activated PXRD patterns

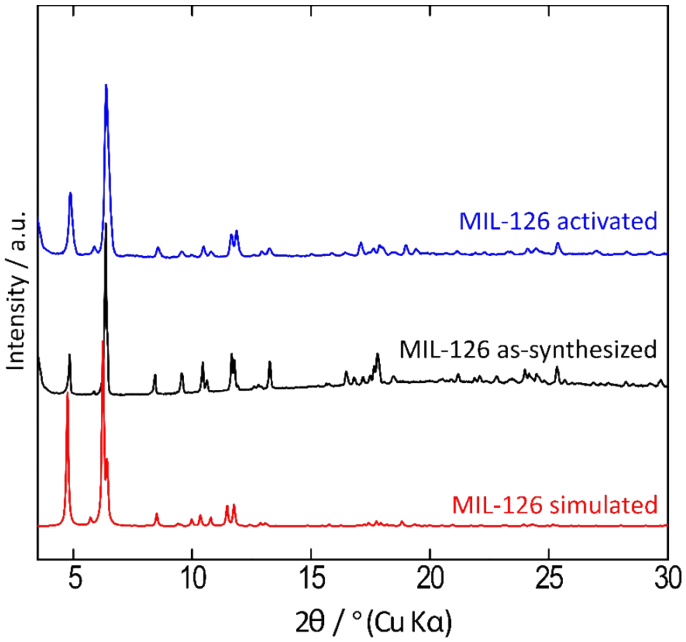

Figure S7. PXRD of simulated MIL-126 compared to as-synthesized and activated PXRD patterns

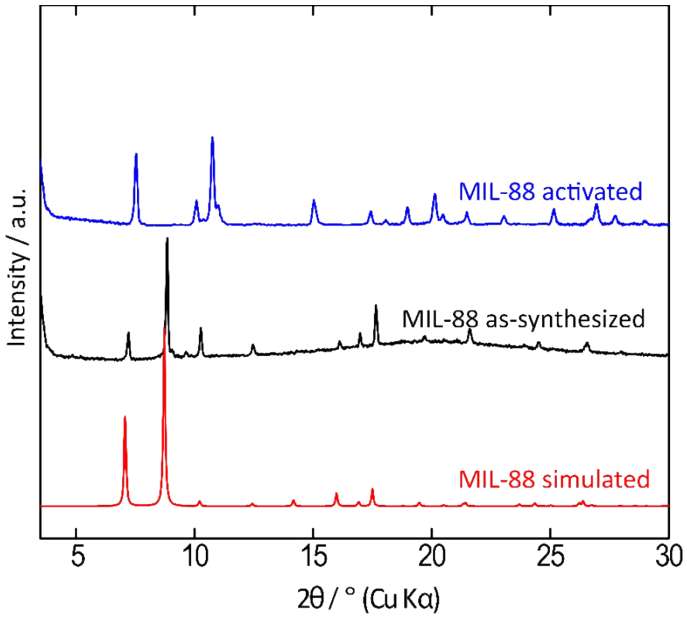

Figure S8. PXRD of simulated MIL-88 compared to as-synthesized and activated PXRD patterns

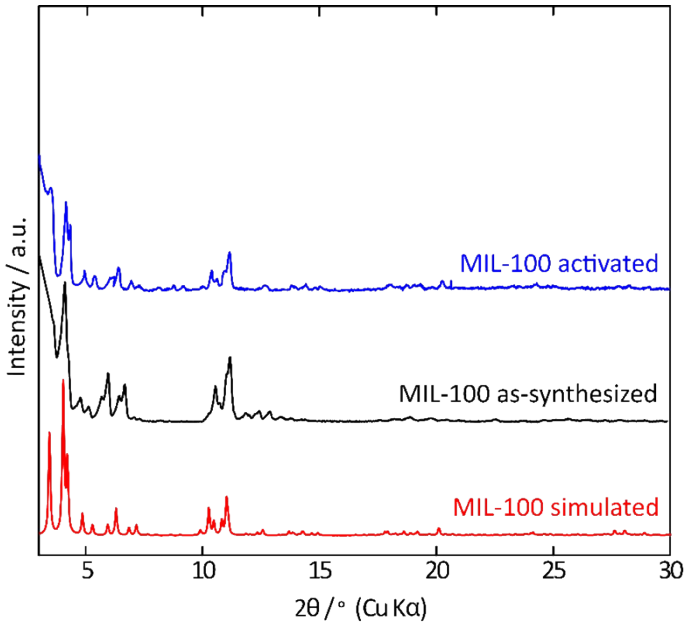

Figure S9. PXRD of simulated MIL-100 compared to as-synthesized and activated PXRD patterns

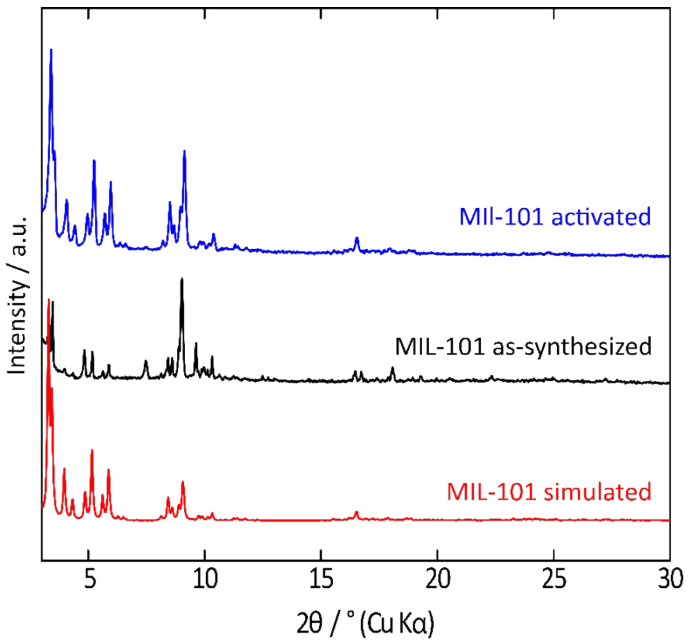

Figure S10. PXRD of simulated MIL-101 compared to as-synthesized and activated PXRD patterns

Section 4: Thermogravimetric Analysis (TGA)

The thermal stability MOF materialswere examined by thermogravimetric analysis. In this measurement, an activated sample of MOF was heated under air flow (60 mL min^{-1}) from 30 to 600 °C with a gradient of 5 °C min^{-1}.

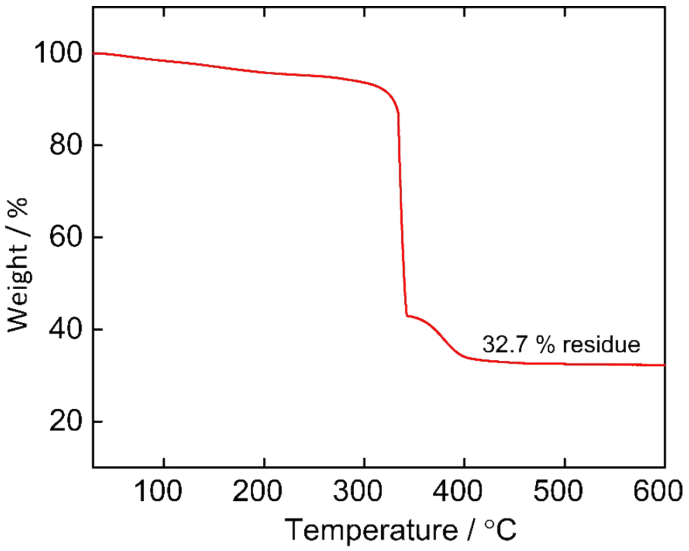

Figure S11. Thermogravimetric analysis of activated MOF-907 under air flow.

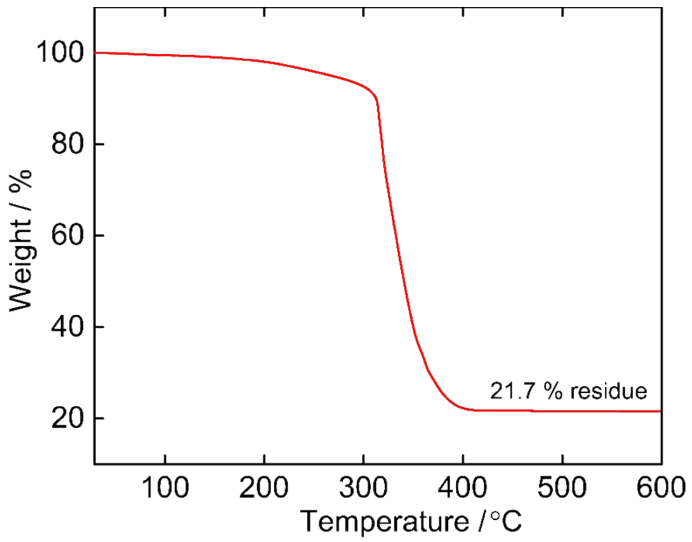

Figure S12. Thermogravimetric analysis of activated MOF-908 under air flow.

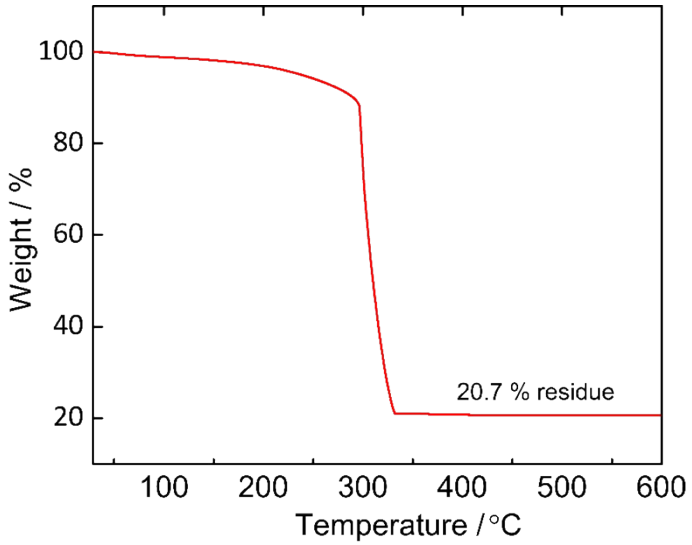

Figure S13. Thermogravimetric analysis of activated MOF-909 under air flow.

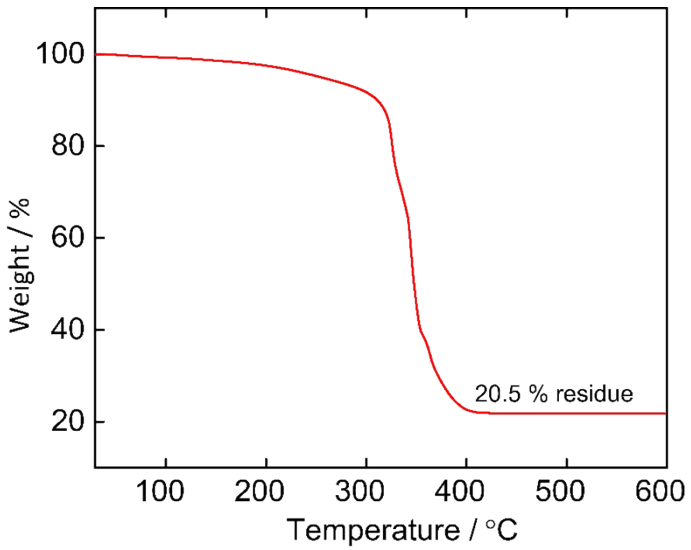

Figure S14. Thermogravimetric analysis of activated PCN-280 under air flow.

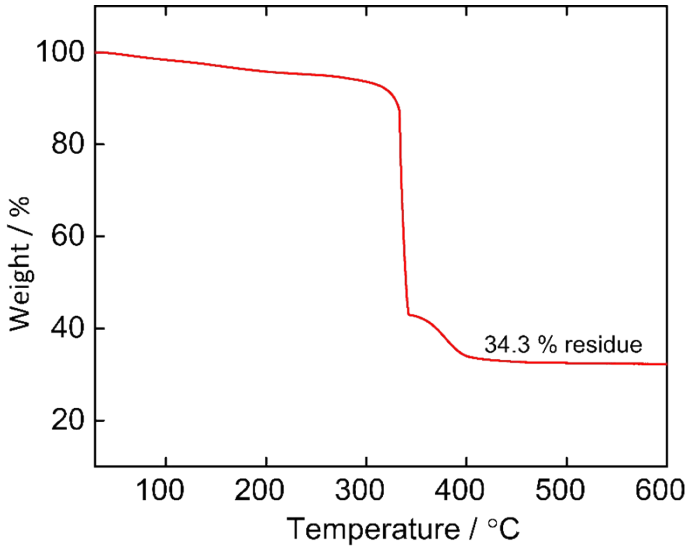

Figure S15. Thermogravimetric analysis of activated PCN-285 under air flow.

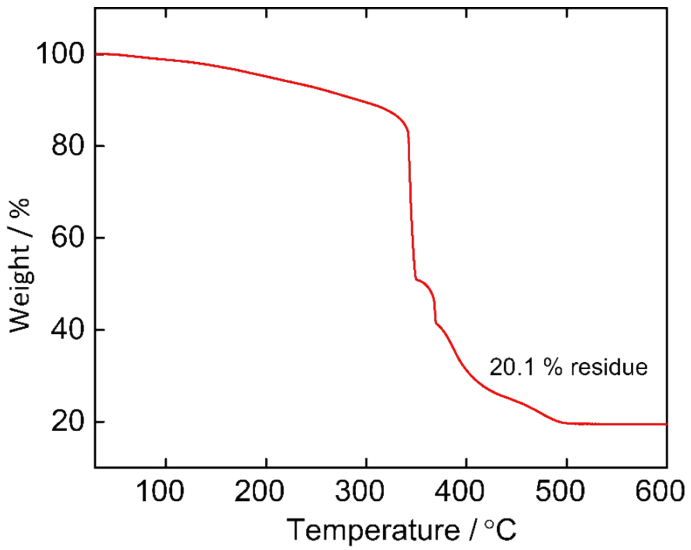

Figure S16. Thermogravimetric analysis of activated MIL-126 under air flow.

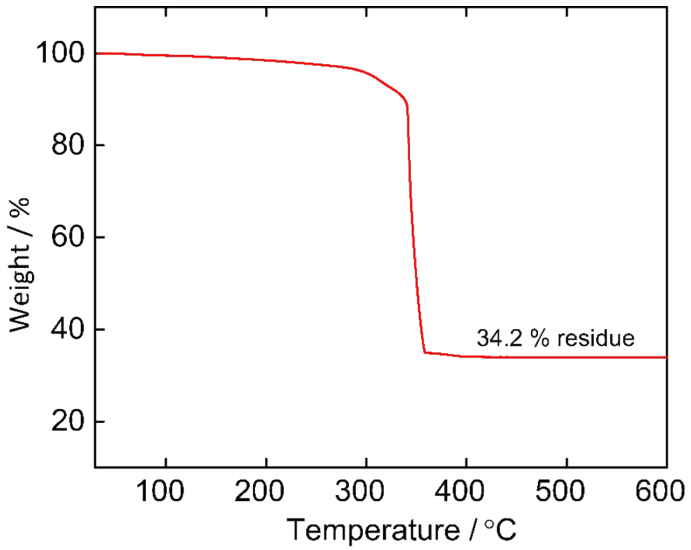

Figure S17. Thermogravimetric analysis of activated MIL-88B under air flow.

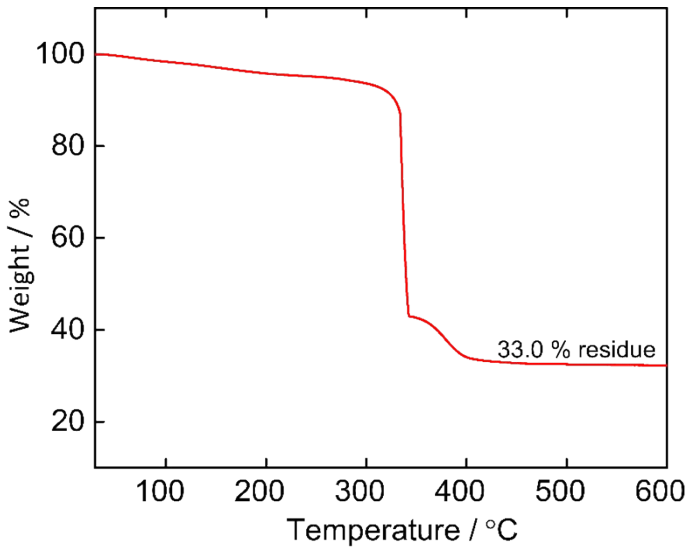

Figure S18. Thermogravimetric analysis of activated MIL-100 under air flow.

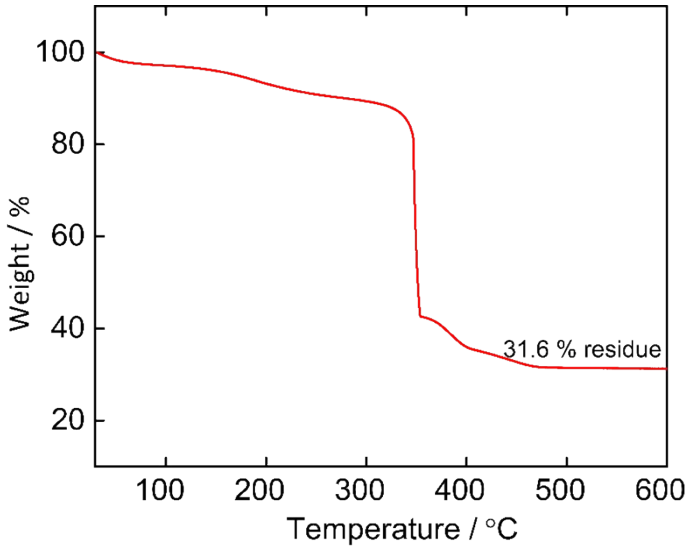

FigureS19. Thermogravimetric analysis of activated MIL-101 under air flow.

Section 5: N_2 adsorption isotherm

The permanent porosity of activated MOF was proven by N_2 adsorption at 77 K, measured by a Micromeritics 3Flex surface characterization analyzer.

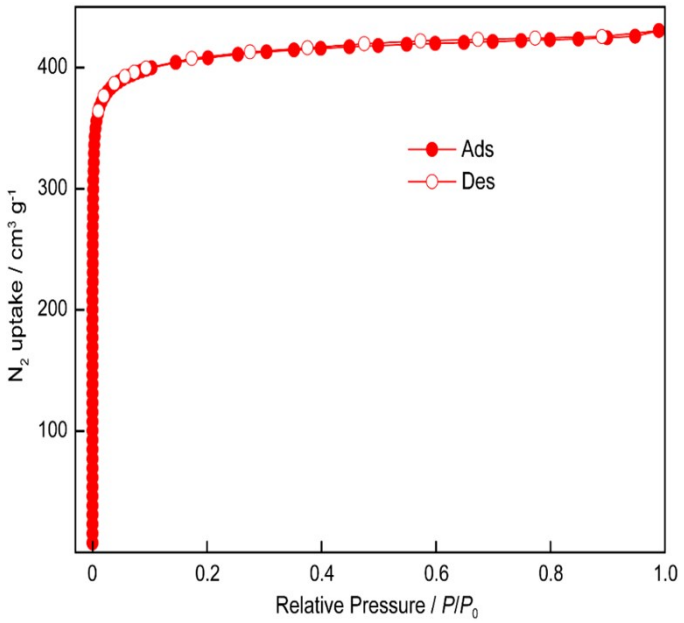

Figure S20. N_2 sorption isotherms of activated MOF-907 at 77 K. The filled and open circles represent the adsorption and desorption branches, respectively. The connecting line is provided as a guide for the eyes.

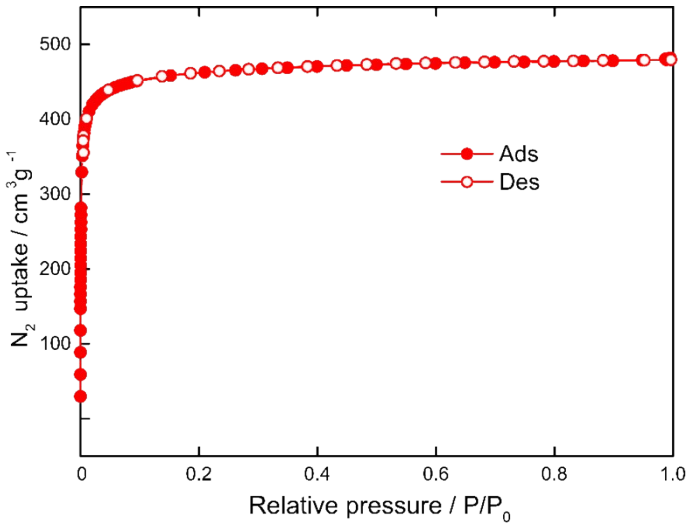

Figure S21. N_2 sorption isotherms of activated MOF-908 at 77 K. The filled and open circles represent the adsorption and desorption branches, respectively. The connecting line is provided as a guide for the eyes.

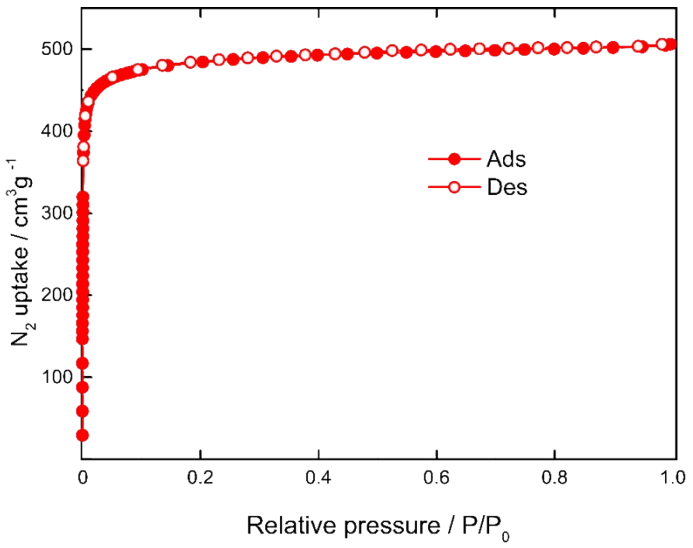

Figure S22. N_2 sorption isotherms of activated MOF-909 at 77 K. The filled and open circles represent the adsorption and desorption branches, respectively. The connecting line is provided as a guide for the eyes

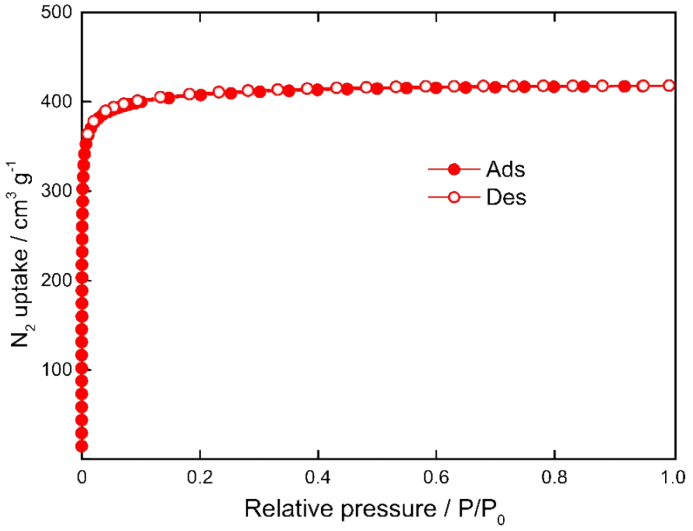

Figure S23. N_2 sorption isotherms of activated PCN-280 at 77 K. The filled and open circles represent the adsorption and desorption branches, respectively. The connecting line is provided as a guide for the eyes.

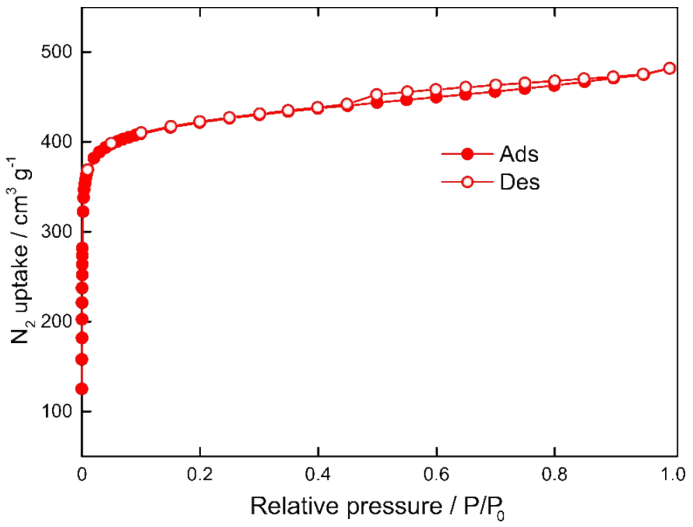

Figure S24. N_2 sorption isotherms of activated PCN-285 at 77 K. The filled and open circles represent the adsorption and desorption branches, respectively. The connecting line is provided as a guide for the eyes.

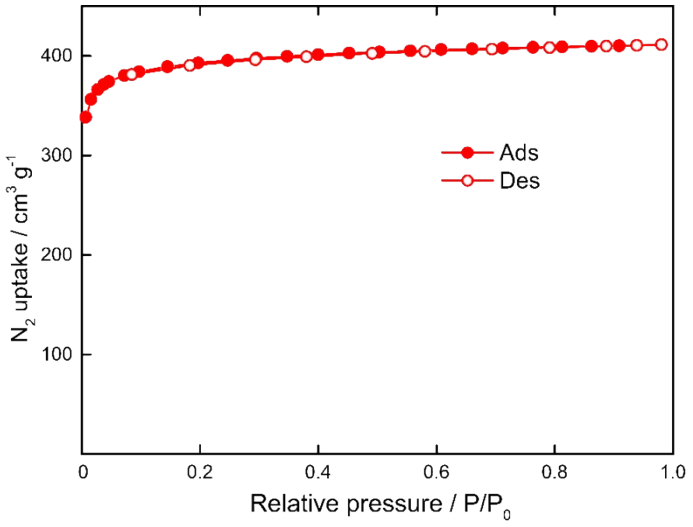

Figure S25. N_2 sorption isotherms of activated MIL-126 at 77 K. The filled and open circles represent the adsorption and desorption branches, respectively. The connecting line is provided as a guide for the eyes.

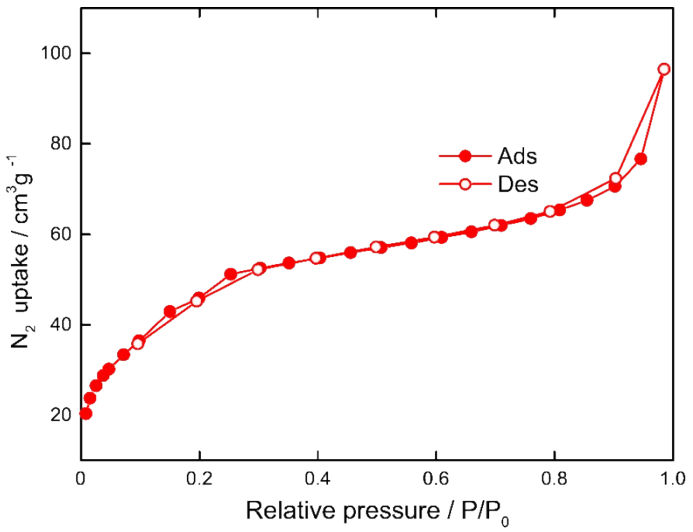

Figure S26. N_2 sorption isotherms of activated MIL-88B at 77 K. The filled and open circles represent the adsorption and desorption branches, respectively. The connecting line is provided as a guide for the eyes.

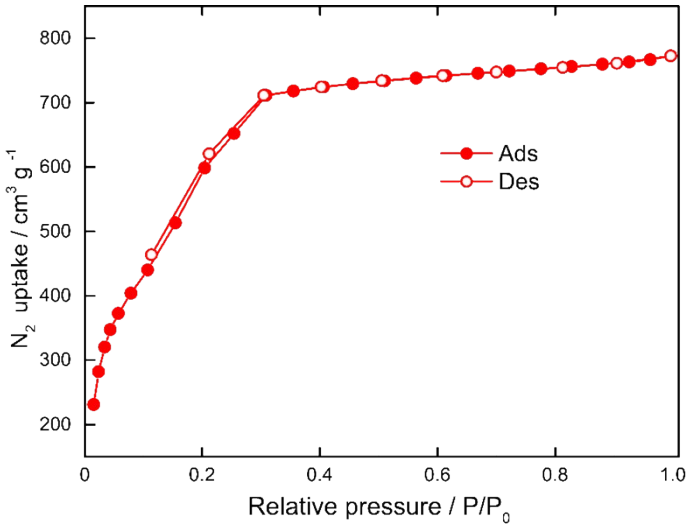

Figure S27. N_2 sorption isotherms of activated MIL-100 at 77 K. The filled and open circles represent the adsorption and desorption branches, respectively. The connecting line is provided as a guide for the eyes.

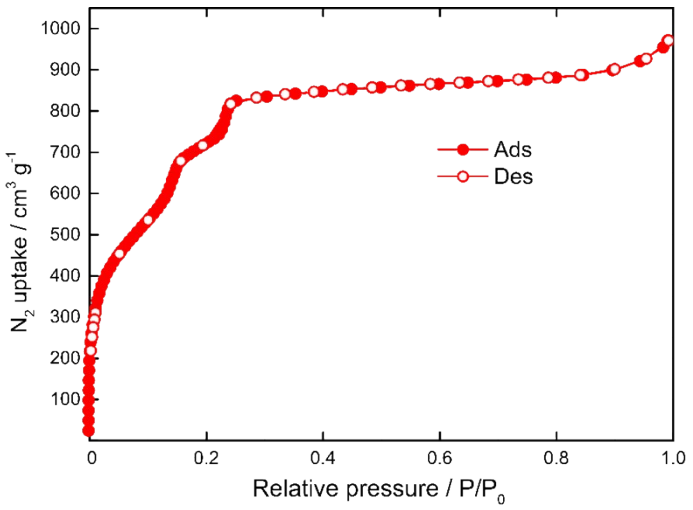

Figure S28. N_2 sorption isotherms of activated MIL-101 at 77 K. The filled and open circles represent the adsorption and desorption branches, respectively. The connecting line is provided as a guide for the eyes.

Table S1. Summary of surface areasand Pore size of Fe-MOFs (cluster Fe^{3+})

Name	**Theoretical value (m^2 g^{-1})**	**Langmuir (m^2 g^{-1})**	**BET (m^2 g^{-1})**	**Pore size Distribution (Å)**	**Ref**
MOF-907	2000	1800	1600	19	[4]
MOF-909	2350	2450	1900	24	[5]
MOF-908	2300	2150	1800	23	[5]
PCN-280	1800	1750	1600	12	[5]
PCN-285	1900	1750	1680	22	[4]
MIL-88B	450	300	164	19	[8,11]
MIL-100	-	2450	2235	25;29	[10]

MIL-101	-	2640	2580	29; 34	[12]
MIL-126	2550	1800	1650	-	[7]

Section S6: Oxidative cyclization reaction data

Table S2. Summary of active site density of mixed linker-based Fe-MOFs

Cat.	**Cell volume**	**Volume (cm^3)**	**Density ($g\ cm^{-3}$)**	**Molar catalyt (10^{-5}mol)**	**Pore size Distribution (Å)**	**Active site density (10^{18} cluster $Å^{-3}$)**	**Space group (N°)**	**Ref**
PCN-285	46525.1	0.047	0.347	1.51009	22	0.909	*R*3 (146)	[6]
MOF-909	43939.4	0.047	0.3569	1.55318	23.5	0.963	*R*3 (146)	[5]
MOF-908	43191.9	0.047	0.3534	1.57888	23	0.979	*R*3 (146)	[5]
MOF-907	87991.1	0.047	0.43	2.10526	19	1.269	*Im*-3*m* (229)	[4]
MIL-101	701861	0.047	0.4659	3.02514	34	1.821	Fd -3m (#227-2)	[13]
PCN-280	21525	0.047	0.731	3.28821	12	1.965	*R*3*m* (160)	[6]
MIL-126	16826.8	0.047	0.752	3.71261	-	2.235	P43212 (#96-1)	[14, 15]
MIL-88	3251.9	0.047	0.7787	2.42279	19	3.018	P63/mmc (#1941)	[16]
MIL-100	394481	0.047	0.7447	3.98804	29	3.241	Fd -3m (#227-2)	[10]

The calculation of active site density (ASD) was followed by the equation: $ASD = \frac{V \times N_{Fe}}{3 \times V_{Cell}}$

Where:

V: Volume of materials

N_{Fe}: Number of Fe atoms in one unit cell

V_{Cell}: Cell volume of materials

Procedure for the synthesis of 2-phenylquinazolin-4(3H)-one

The reaction included benzyl alcohol (1.5 mmol), 2-aminobenzamide (0.5 mmol), Fe-MOF (4.2 mol%) and tert-butyl hydroperoxide (TBHP) (70% in water) (2 mmol)was heated by microwave irradiation system at 120 ^{o}C for 1.5 minutes. After reaction completion, the mixture was dissolved with ethyl acetate and centrifuged to remove catalyst. The pure product was refined by column chromatography (9:1 ratio of n-hexane/ethyl acetate). 2-Phenylquinazolin-4(3H)-one compound was confirmed via melting point, FT-IR, ^{1}H and ^{13}C NMR, GC-MS. For the reusable survey, the catalyst was washed with ethyl acetate (3 x 2 mL) and dried at 80 ^{o}C for next cycle.

Table S3. Effects of the other catalyst on the synthesis of 2-phenylquinazolin-4(3*H*)-one

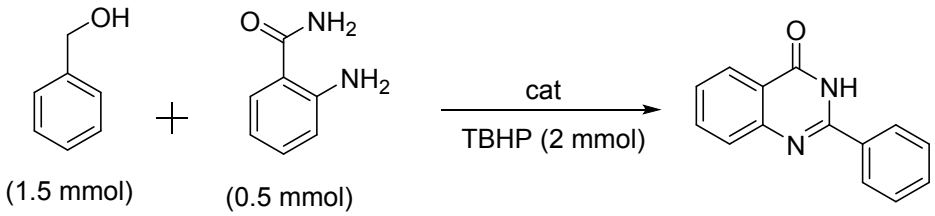

Entry[a]	Cat.	Volume (mL)	Density (g/mL)	Mass (mg)	GC Yield (%)
1	PCN-285	0.047	0.347	16.31	95
2	MOF-909	0.047	0.357	16.78	13
3	MOF-908	0.047	0.353	16.59	40
4	MOF-907	0.047	0.430	20.21	95
5	MIL-101	0.047	0.466	21.90	95
6	PCN-280	0.047	0.731	34.36	45
7	MIL-126	0.047	0.752	35.34	18
8	MIL-88B	0.047	0.779	36.61	40

9	MIL-100	0.047	0.745	35.02	95
10	HKUST-1	0.047	1.143	53.72	30
11	ZIF-8	0.047	1.037	48.74	20
12	MOF-177	0.047	0.423	19.88	8

[a] Reaction condition: benzyl alcohol (1.5 mmol, 108 mg), 2-aminobenzamide (0.5 mmol, 68 mg), TBHP (2 mmol, 277 μL), were heated by microwave irradiation system at 120°C in 1.5 minutes.

Table S4. Effects of MOF-907, MIL-101, MIL-100, PCN-285 on the synthesis of 2-2-methyl-2-phenyl-2,3-dihydroquinazolin-4(1*H*)-one

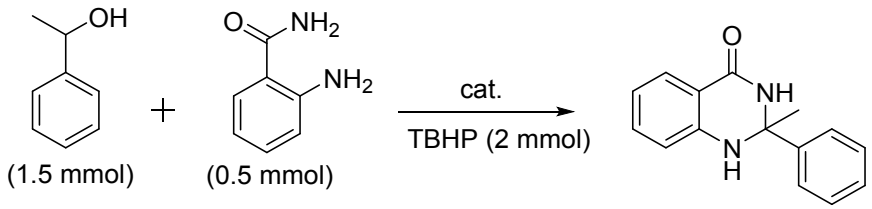

Entry[a]	Cat.	Volume (mL)	Density (g/mL)	Mass (mg)	GC Yield (%)
1	PCN-285	0.047	0.347	16.3	8
2	MOF-907	0.047	0.430	20	15
3	MIL-101	0.047	0.466	21.9	0
4	MIL-100	0.047	0.745	35	0

[a] Reaction condition: 1-phenylethanol (1.5 mmol, 183 mg), anthranilamide (0.5 mmol, 68 mg), TBHP (2 mmol, 277 μL), were heated by microwave irradiation system at 120°C in 1.5 minutes.

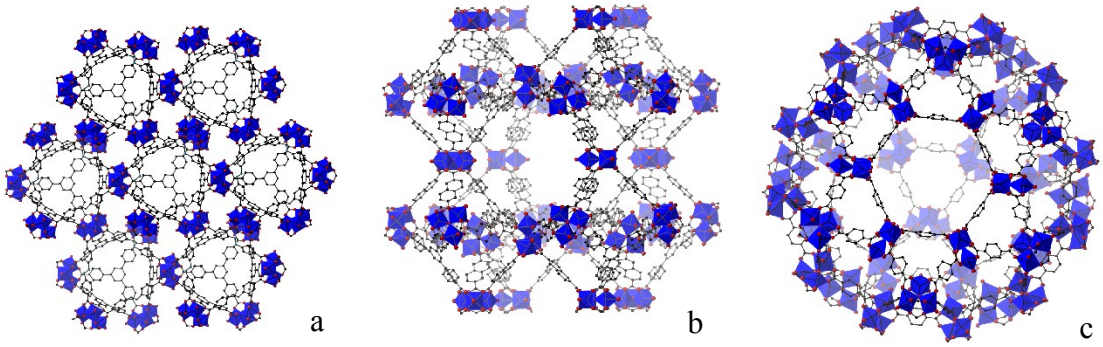

Figure S29. Structuresof MOF materials a)PCN-285 have structure meso MOFs b) MOF-907 MOF-907 possesses 1-D interconnected channels. C) MIL-101have structure Cage-type meso MOFs.Atom colors: Fe: blue polyhedral. C: black, and O: red. All H atoms are omitted for clarity.

Table S5. Optimization of reaction condition on the synthesis of 2-phenylquinazolin-4(3H)-one.

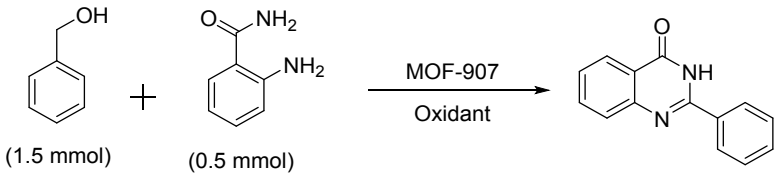

Entry	MOF-907 catalyst (mol%)	Oxidant	Molar of oxidant	Reaction Condition °C (min)	GC Yield (%)
1	0	TBHP	2.0	120 (15)	0
2	2.1	TBHP	2.0	120 (15)	18
3	2.7	TBHP	2.0	120 (15)	24
4	3.2	TBHP	2.0	120 (15)	47
5	3.6	TBHP	2.0	120 (15)	60
6	4.2	TBHP	2.0	120(15)	95
7	4.2	TBHP	2.0	60 (15)	0
8	4.2	TBHP	2.0	70 (15)	0
9	4.2	TBHP	2.0	80 (15)	Trace
10	4.2	TBHP	2.0	100 (15)	60
11	4.2	TBHP	2.0	110 (15)	65
12	4.2	TBHP	2.0	120(10)	95
13	4.2	TBHP	2.0	120(5.0)	93
14	4.2	TBHP	2.0	120(2.0)	95
15	4.2	TBHP	2.0	120(1.5)	95
16	4.2	TBHP	2.0	120 (1.0)	83
17	4.2	TBHP	2.0	120(0.5)	55
18	4.2	TBHP	1.5	120(1.5)	83

19	4.2	TBHP	1.0	120(1.5)	50
20	4.2	-	-	120(1.5)	0
21	4.2	H_2O_2	2.0	120(1.5)	0
22	4.2	DTBP	2.0	120(1.5)	70
23	4.2	$K_2S_2O_8$	2.0	120 (1.5)	80

Table S6. Synthesis of 2-phenylquinazolin-4(3*H*)-one and 2,3-dihydroquinazolin-4-one derivatives

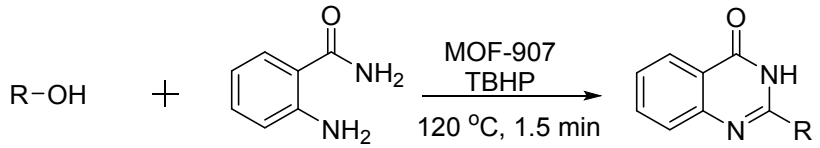

Entry[a]	Alcohols	Products	Yield[b] (%)	TOF
1	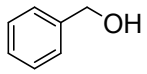	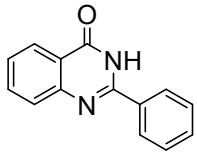	95[a]	902.5
2	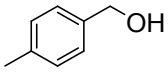	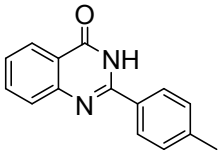	95[a]	902.5
3	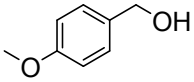	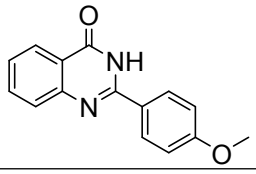	88[a]	835.9
4	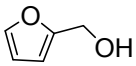	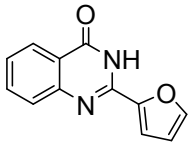	85[a]	807.4
5	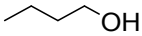	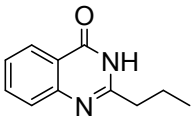	70[a]	664.9
6	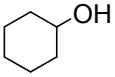	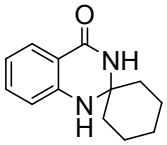	95[b]	67.7

7	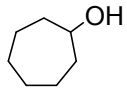	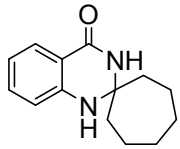	70[b]	49.9
8	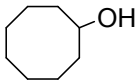	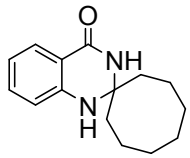	40[b]	22.8
9		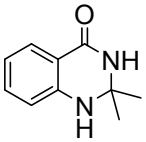	50[b]	35.6
10	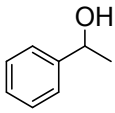	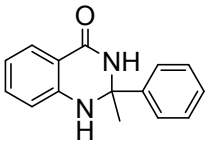	25[b]	10.7
Reaction condition: 2-aminobenzamide (0.5 mmol, 68 mg), TBHP (2 mmol, 277 μL) were heated by microwave irradiation system at 120 °C. Holding time microwave irradiation was 1.5 min[a] and 20 min[b]				

Equation 1: The calculation formula of TOF

$$TOF\left(h^{-1}\right) = \frac{moles\ of\ product}{moles\ of\ cat.\ \times h}$$

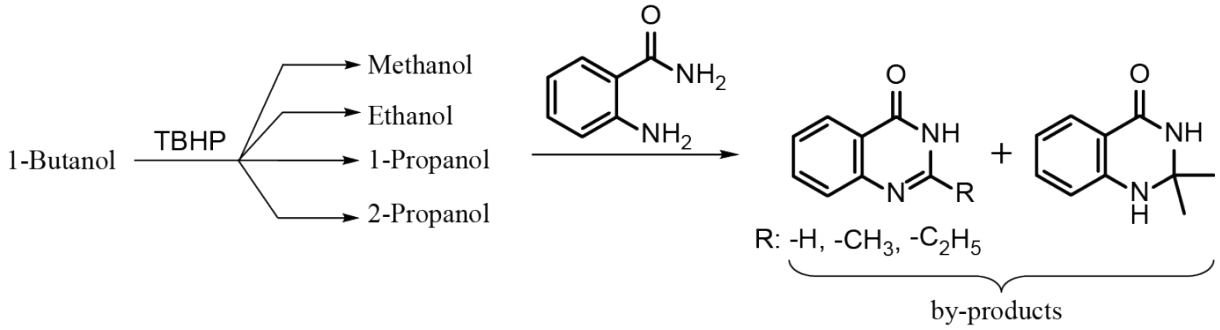

Scheme S1. The by-product formation of the reaction between 1-butanol and 2-aminobenzamide

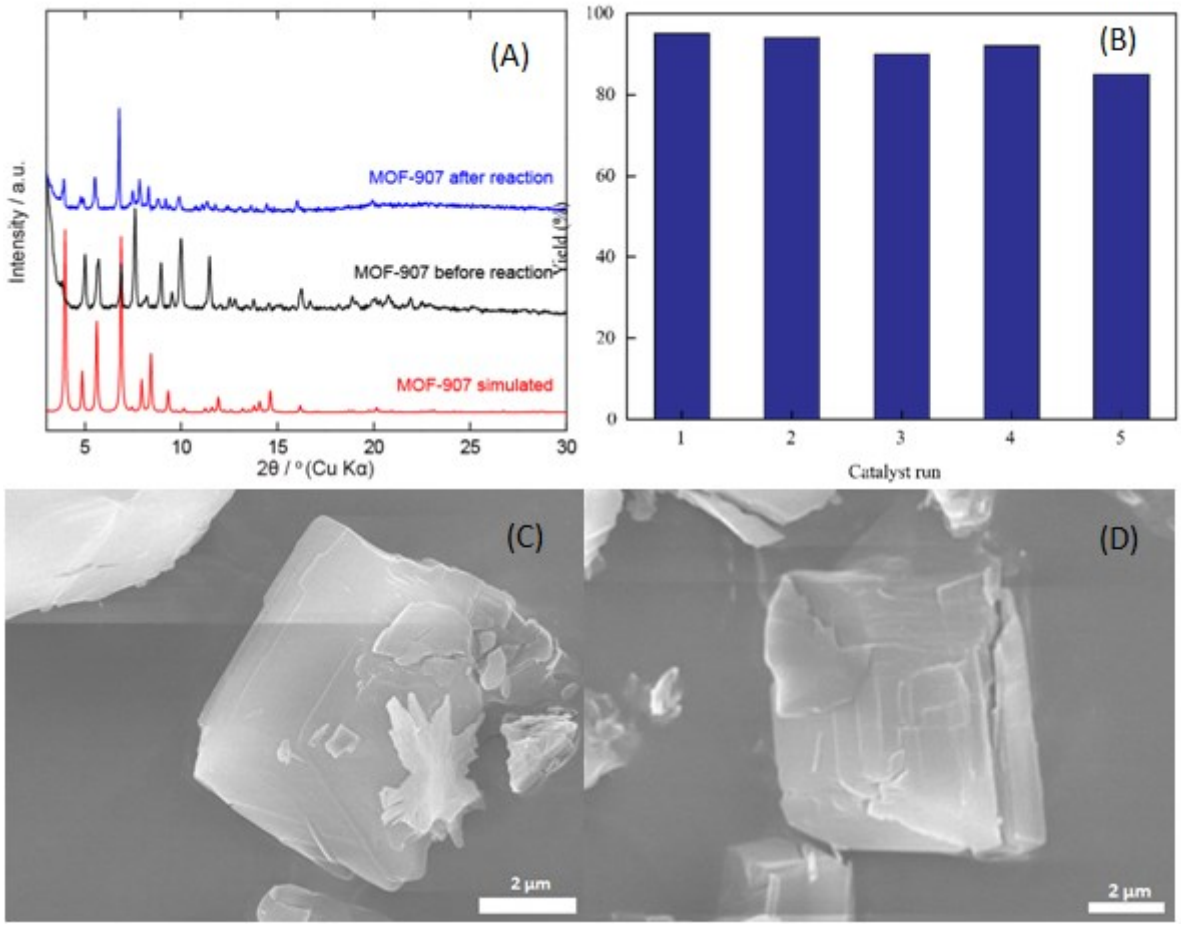

Figure S30.(A) P-XRD analysis of MOF-907 before (blue) and after (black) reaction in comparison to the simulated pattern. (B) Reusable ability of MOF-907. (C), (D) SEM images of MOF-907before and after the catalysis.

Section 7. IR, NMR data of quinazolin-4(3H)-ones and 2,3-dihydroquinazolin-4-ones

2-phenylquinazolin-4(3*H*)-one

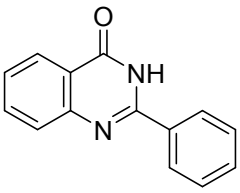

Yield: 95%

Color: White solid

Melting point: 230-232°C

FT-IR (ATR, 4000 – 600 cm^{-1}): 3167, 2921, 2851, 1660, 1597, 1288.

^{1}H NMR (500 MHz, DMSO- d_6):δ 12.48 (s, 1H), 8.15 – 8.11 (m, 3H), 7.85 – 7.82 (m, 1H), 7.74 (d,J = 8.0 Hz, 1H), 7.60 – 7.51 (m, 4H).

^{13}C NMR (125 MHz, DMSO- d_6): δ 162.8, 152.9, 149.1, 135.1, 133.0, 131.8, 129.1, 128.1, 127.7, 127.1, 126.2, 121.1.

GC-MS (EI, 70 eV) *m/z*: 222 ([M]$^+$)

2-(*p*-tolyl)quinazolin-4(3*H*)-one

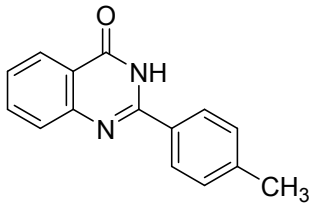

Yield: 95%

Color: White solid

Melting point: 231-233°C

FT-IR (ATR, 4000 – 600 cm^{-1}):3173, 3065, 2920, 2852, 1657, 1599, 1285.

^{1}H NMR (500 MHz, DMSO- d_6):δ 12.4 (s, 1H), 8.13 (dd, J = 8.0, 1.5 Hz, 1H), 8.03 (d, J = 8.0 Hz, 2H), 7.82 (td, J = 8.0, 1.5 Hz, 1H), 7.72 (d, J = 8.0 Hz, 1H), 7.52 – 7.48 (m, 1H), 7.34 (d, J = 8.0 Hz, 2H), 2.37 (s, 3H).

^{13}C NMR (125 MHz, DMSO- d_6): δ 162.8, 152.7, 149.1, 142.0, 135.1, 130.1, 129.6, 128.0, 127.7, 126.9, 126.2, 125.0, 23.1.

GC-MS (EI, 70 eV) *m/z*: 236 ([M]$^+$)

2-(4-methoxyphenyl)quinazolin-4(3*H*)-one

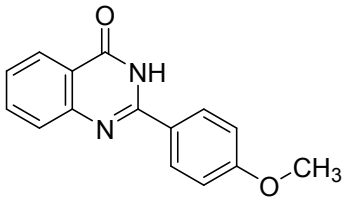

Yield: 88%

Color: White solid

Melting point: 240-243°C

FT-IR (ATR, 4000 – 600 cm^{-1}): 3153,3064, 2918, 2850, 1672, 1598, 1244, 1029.

^{1}H NMR (500 MHz, DMSO- *d$_6$*):δ 12.4 (s, 1H), 8.19 (d,*J* = 8.5 Hz,2H), 8.13 (dd,*J* = 8.0, 1.0 Hz,1H), 7.83 – 7.79 (m, 1H), 7.70 (d,*J* = 8.0 Hz,1H), 7.50 – 7.46 (m,1H), 7.10 – 7.08 (m, 2H), 3.85 (s, 3H).

^{13}C NMR (125 MHz, DMSO- *d$_6$*): δ 162.8, 162.3, 152.4, 149.3, 135.0, 129.3, 127.7, 126.6, 126.3, 125.3, 121.2, 114.5, 55.9.

GC-MS (EI, 70 eV) *m/z*: 252 ([M]$^+$)

2-(furan-2-yl)quinazolin-4(3*H*)-one

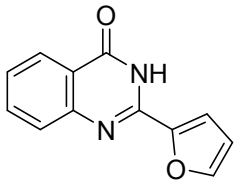

Yield: 85%

Color: White solid

Melting point: 215-217°C

FT-IR (ATR, 4000 – 600 cm^{-1}): 3123, 2954, 2920, 2852, 1676, 1600, 1459, 1266, 1021.

^{1}H NMR (500 MHz, DMSO- *d$_6$*):δ 12.5 (s, 1H), 8.13 (dd, *J* = 8.0, 1.0 Hz, 1H), 8.00 (d, *J* = 1.0 Hz, 1H), 7.83 – 7.80 (m, 1H), 7.69 (d, *J* = 8.0 Hz, 1H), 7.63 (d, *J* = 3.0 Hz, 1H), 7.51 – 7.48 (m, 1H), 6.75 (dd, *J* = 3.0, 1.0 Hz, 1H).

^{13}C NMR (125 MHz, DMSO- *d$_6$*): δ 162.0, 149.1, 147.0, 146.6, 144.5, 135.1, 127.7, 127.0, 126.4, 121.6, 115.0, 113.0.

GC-MS (EI, 70 eV) *m/z*:212 ([M]$^+$)

2-propylquinazolin-4(3*H*)-one

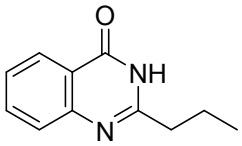

Yield: 70%

Color: White solid

Melting point: 192-194°C

FT-IR (ATR, 4000 – 600 cm^{-1}): 3166, 3033, 2961, 2920, 1672, 1617, 1501, 1251.

^{1}H NMR (500 MHz, DMSO- d_6):δ 12.1 (s, 1H), 8.07 (dd, J = 8.0, 1.0 Hz, 1H), 7.78 – 7.74 (m, 1H), 7.58 (d, J = 8.0 Hz, 1H), 7.46 – 7.43 (m, 1H), 2.57 (t, J = 7.5 Hz, 2H), 1.74 (sex, J = 7.5 Hz, 2H), 0.93 (t, J= 7.5 Hz, 3H).

^{13}C NMR (125 MHz, DMSO- d_6): δ 162.3, 157.8, 149.4, 134.7, 127.3, 126.4, 126.1, 121.3, 36.8, 20.7, 13.9.

GC-MS (EI, 70 eV) *m/z*:188 ([M]$^+$)

2-methyl-2-phenyl-2,3-dihydroquinazolin-4(1*H*)-one

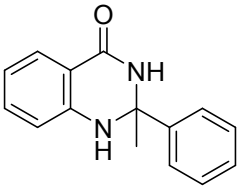

Yield: 25%

Color: Brown solid

Melting point: 223-225°C

IR (ATR, 4000-600 cm^{-1}): 3398, 3177, 2927, 1657, 1610, 1489, 1150, 1025.

^{1}H NMR (500 MHz, DMSO- d_6):δ 8.73 (s, 1H), 7.60 (s, 1H), 7.48 – 7.45 (m, 3H), 7.26 (t,J = 8.0 Hz, 2H), 7.20 – 7.14 (m, 2H), 6.75 (d, J = 8.0 Hz, 1H), 6.58 – 6.54 (m, 1H), 1.62 (s, 3H).

^{13}C NMR (125 MHz, DMSO- d_6): δ 164.2, 148.1, 147.6, 133.7, 128.4, 127.7, 127.5, 125.6, 117.3, 115.5, 114.7, 70.6, 31.2.

GC-MS (EI, 70 eV) *m/z*:238 ([M]$^+$)

1'*H*-spiro[cyclohexane-1,2'quinazolin]-4'(3'*H*)-one

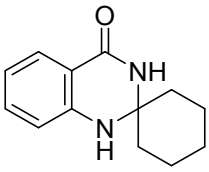

Yield: 95%

Color: White solid

Melting point: 217-220°C

IR (ATR 4000-600 cm^{-1}): 3360, 3164, 2924, 1642, 1604, 1473, 1034.

^{1}H NMR (500 MHz, DMSO- d_6):δ 7.87 (s, 1H), 7.54 (dd, J = 8.0, 1.5 Hz, 1H), 7.19 (td, J = 8.0, 1.5, 1H), 6.78 (d, J = 8.0 Hz, 1H), 6.61 – 6.58 (m, 2H), 1.75 – 1.70 (m, 2H), 1.61 – 1.48 (m, 6H), 1.44 – 1.38 (m, 1H), 1.27 – 1.19 (m, 1H).

^{13}C NMR (125 MHz, DMSO- d_6):δ 163.6, 147.2, 133.6, 127.6, 116.9, 115.0, 114.9, 68.3, 37.6, 25.1, 21.4.

GC-MS (EI, 70 eV) *m/z*:216 ([M]$^{+}$)

1'*H*-spiro[cycloheptane-1,2'-quinazolin]-4'(3'*H*)-one

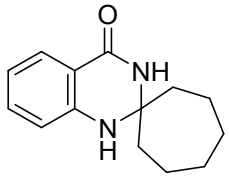

Yield: 70%

Color: White solid

Melting point: 219-222°C

IR (ATR 4000-600 cm^{-1}): 3332, 3173, 2922, 1609, 1487, 1038.

^{1}H NMR (500 MHz, DMSO- d_6):δ 7.98 (s, 1H), 7.52 (dd, J = 8.0, 1.5 Hz, 1H), 7.20 – 7.16 (m, 1H), 6.70 –6.98 (m, 2H); 6.60 – 6.56 (m, 1H), 1.91 – 1.80 (m, 4H), 1.49 (s, 8H).

^{13}C NMR (125 MHz, DMSO- d_6):δ 163.4, 147.2, 133.6, 127.53, 116.8, 114.8, 72.4, 41.5, 29.6, 21.3.

GC-MS (EI, 70 eV) *m/z*:230 ([M]$^{+}$)

1'*H*-spiro[cyclooctane-1,2'-quinazolin]-4'(3'*H*)-one

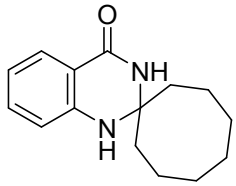

Yield: 40%

Color: White solid

Melting point: 219-223°C

IR (ATR 4000-600 cm^{-1}): 3354, 3222, 2916, 1643, 1633, 1482, 1421, 1011.

^{1}H NMR (500 MHz, DMSO- d_6): δ 7.92 (s, 1H), 7.52 (dd, J = 8.0, 1.5 Hz, 1H), 7.20 – 7.16 (m, 1H), 6.71 (d, J = 8.0 Hz, 1H), 6.60 – 6.56 (m, 2H), 1.91 – 1.80 (m, 4H), 1.52 – 1.49 (m, 10H).

^{13}C NMR (125 MHz, DMSO- d_6):δ 163.4, 147.3, 133.6, 127.5, 116.7, 114.8, 71.8, 36.1; 28.2, 24.6, 21.2.

GC-MS (EI, 70 eV) *m/z*:244 ([M]$^{+}$)

2,2-dimethyl-2,3-dihydroquinazolin-4(1*H*)-one

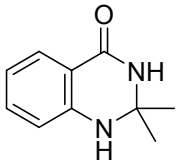

Yield: 50%

Color: White solid

Melting point: 195-198°C

IR (ATR 4000-600 cm^{-1}): 3326, 3174, 2924, 1606, 1478, 1424, 1025.

^{1}H NMR (500 MHz, DMSO- d_6):δ 7.89 (s, 1H), 7.55 (dd, J = 8; 1.5 Hz, 1H), 7.21 – 7.18 (m, 1H), 6.62 – 6.58 (m, 3H), 1.36 (s, 6H).

^{13}C NMR (125 MHz, DMSO- d_6):δ 163.5, 147.5, 133.6, 127.64, 116.9, 114.7, 114.3, 67.3, 29.47.

GC-MS (EI, 70 eV) *m/z*:176 ([M]$^{+}$)

Section 8. Copies of ^{1}H , ^{13}C NMR and HRMS spectra of all products

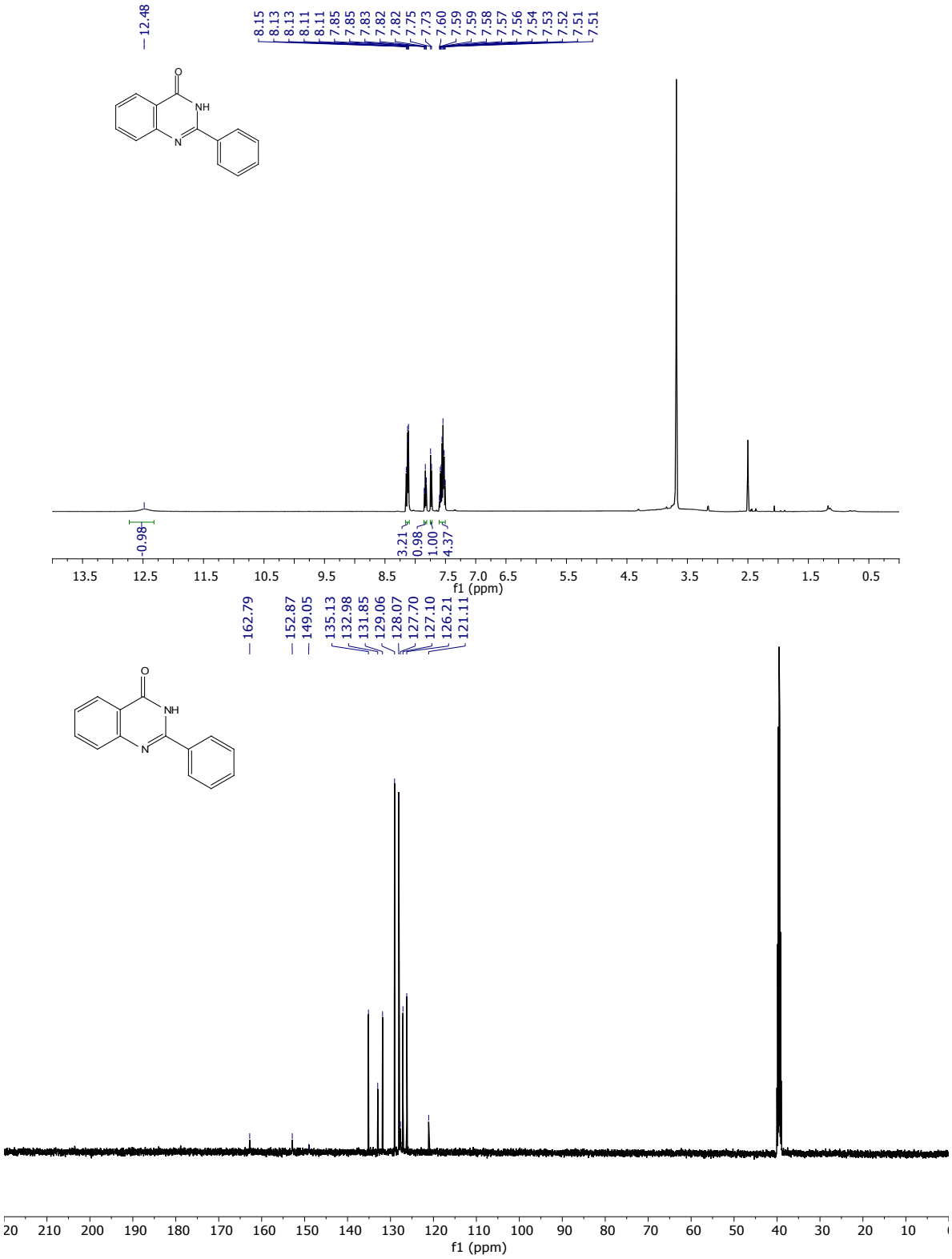

Figure S31. ^{1}H (top) and ^{13}C (bottom) NMR spectra of2-phenylquinazolin-4(3*H*)-one

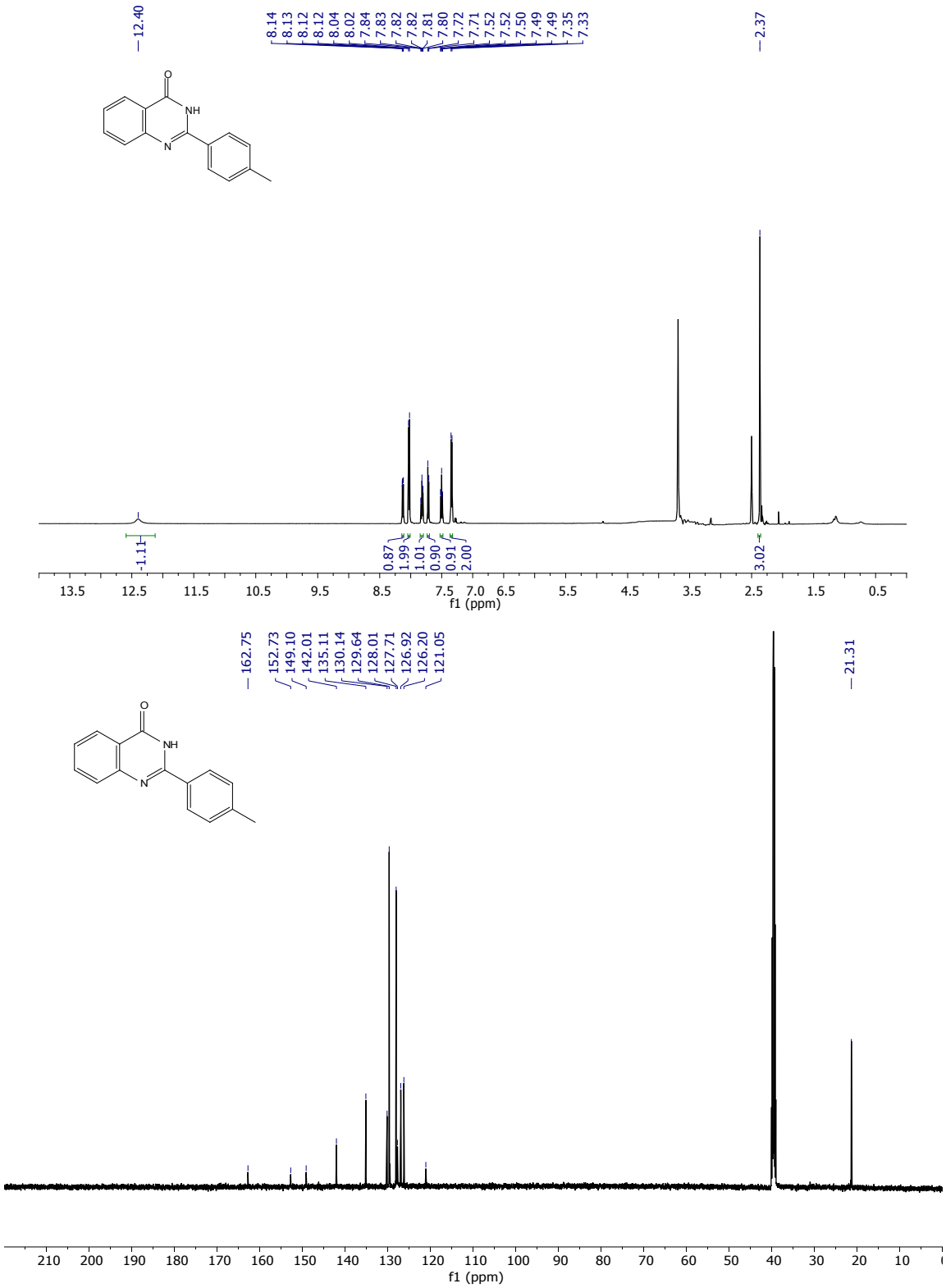

Figure S32. ^{1}H (top) and ^{13}C (bottom) NMR spectra of2-(*p*-tolyl)quinazolin-4(3*H*)-one

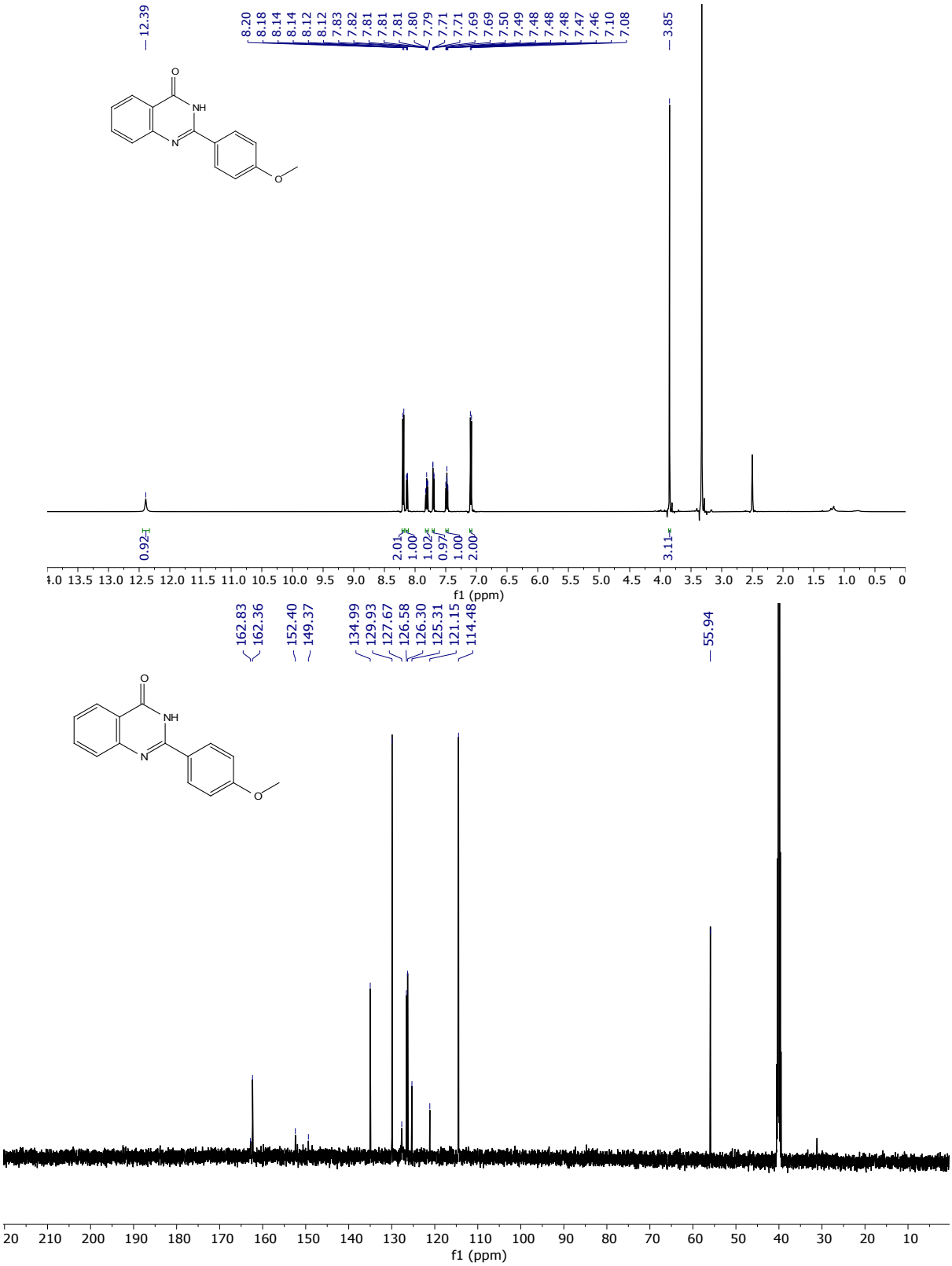

Figure S33. ^{1}H (top) and ^{13}C (bottom) NMR spectra of2-(4-methoxyphenyl)quinazolin-4(3*H*)-one

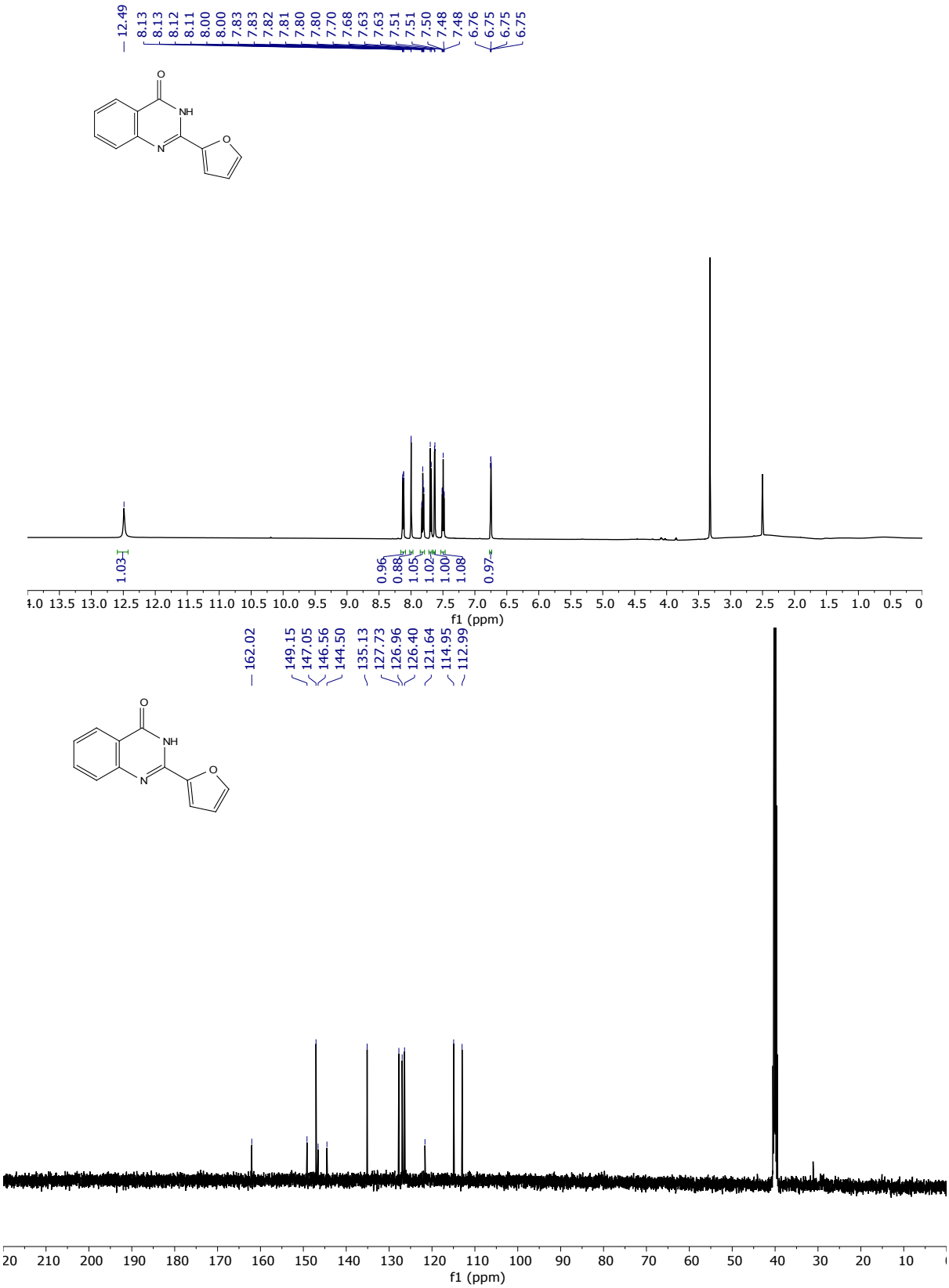

Figure S34. ^{1}H (top) and ^{13}C (bottom) NMR spectra of2-(furan-2-yl)quinazolin-4(3*H*)-one

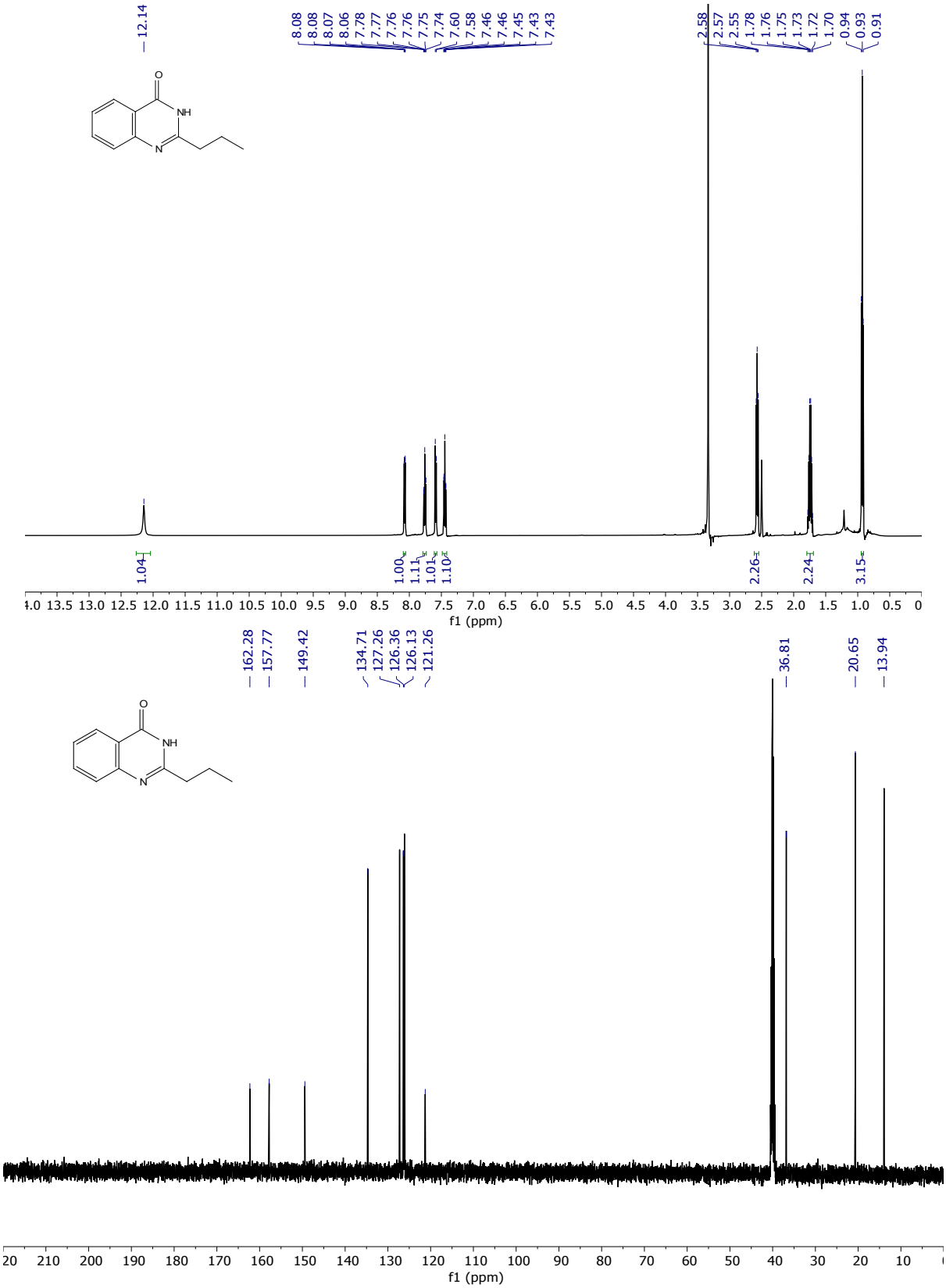

Figure S35. ^{1}H (top) and ^{13}C (bottom) NMR spectra of 2-propylquinazolin-4(3*H*)-one

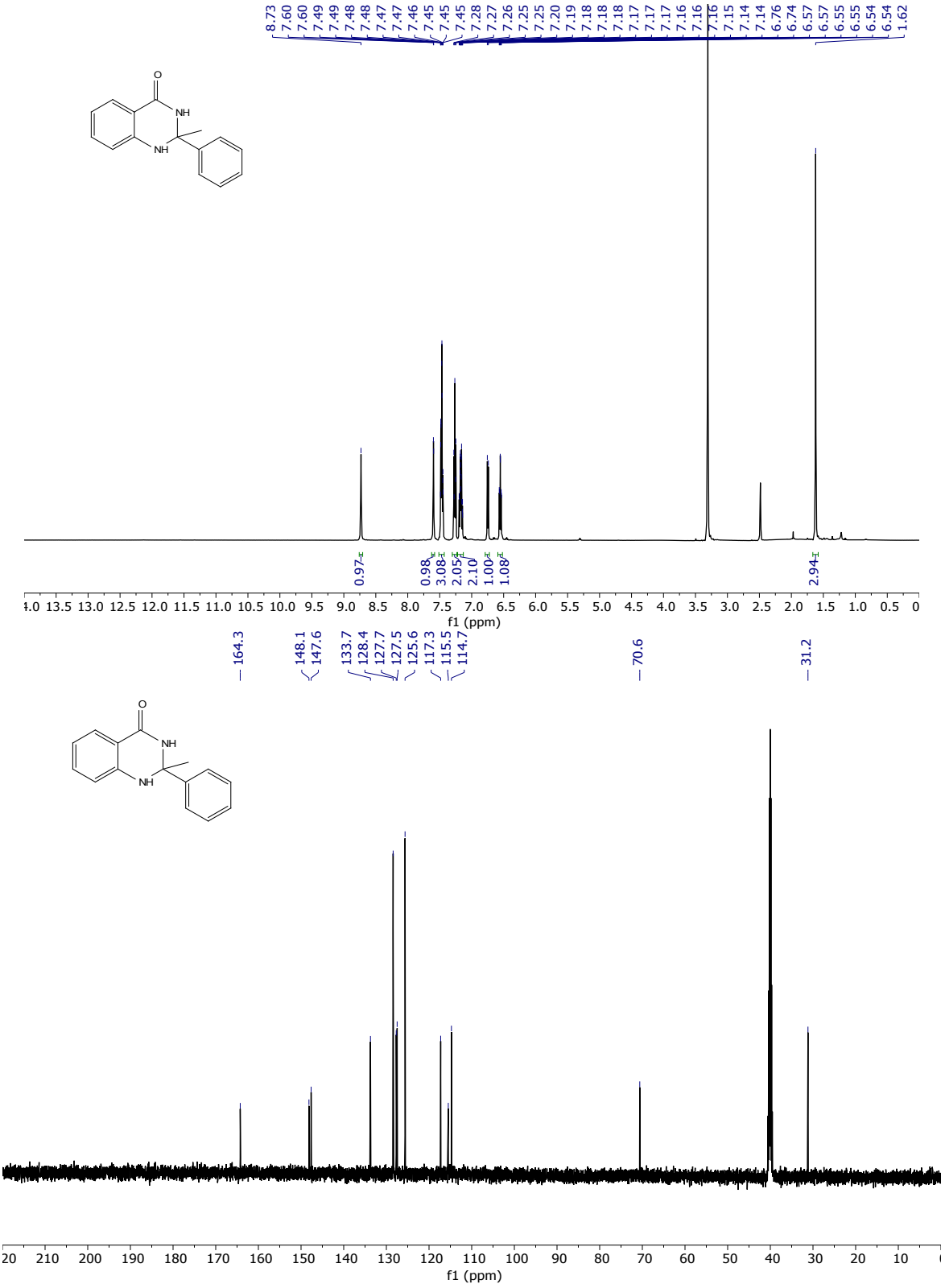

Figure S36. ^{1}H (top) and ^{13}C (bottom) NMR spectra of 2-methyl-2-phenyl-2,3-dihydroquinazolin-4(1*H*)-one

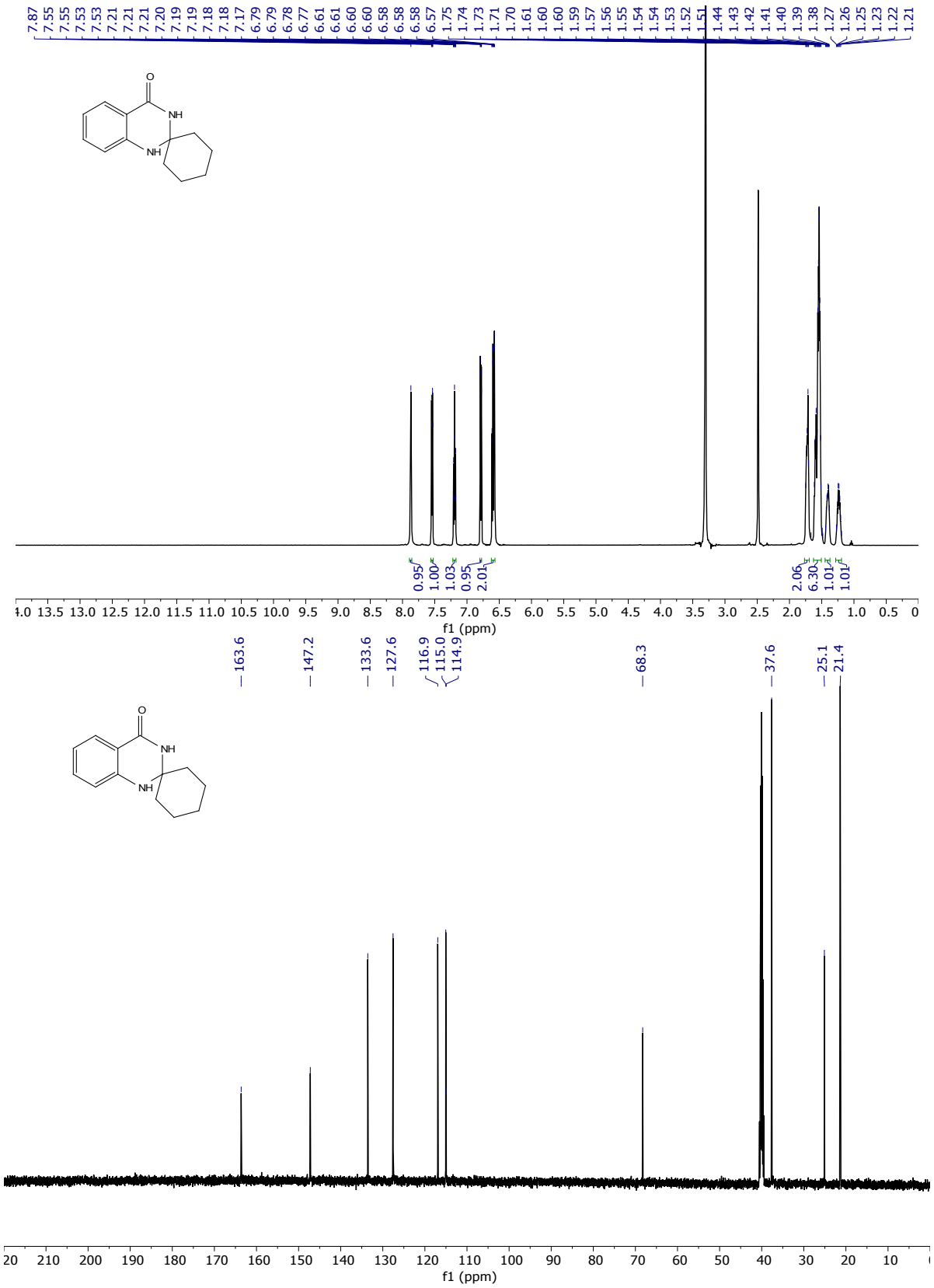

Figure S37. ^{1}H (top) and ^{13}C (bottom) NMR spectra of 1'*H*-spiro[cyclohexane-1,2'-quinazolin]-4'(3'*H*)-one

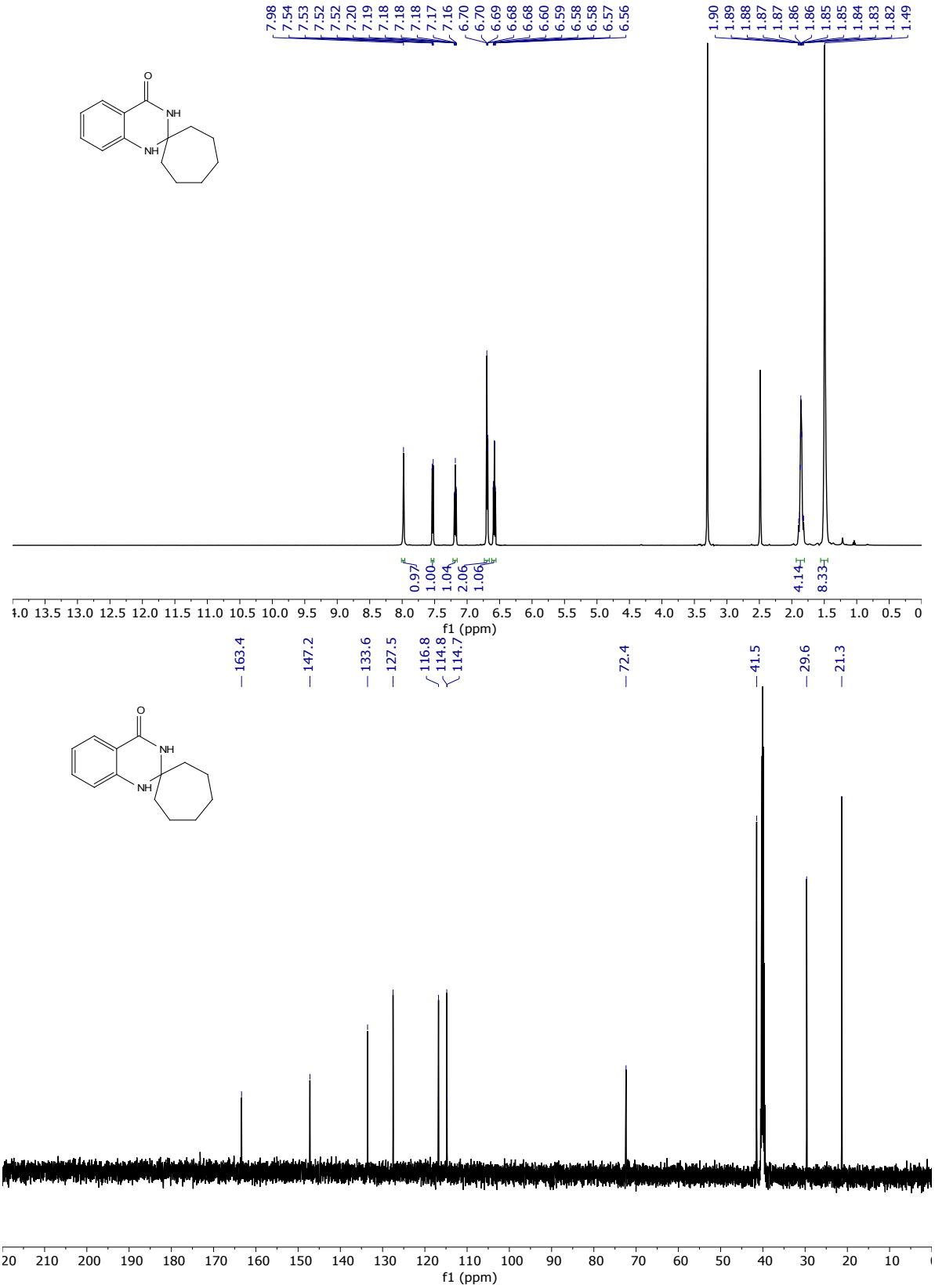

Figure S38. ^{1}H (top) and ^{13}C (bottom) NMR spectra of 1'*H*-spiro[cycloheptane-1,2'-quinazolin]-4'(3'*H*)-one

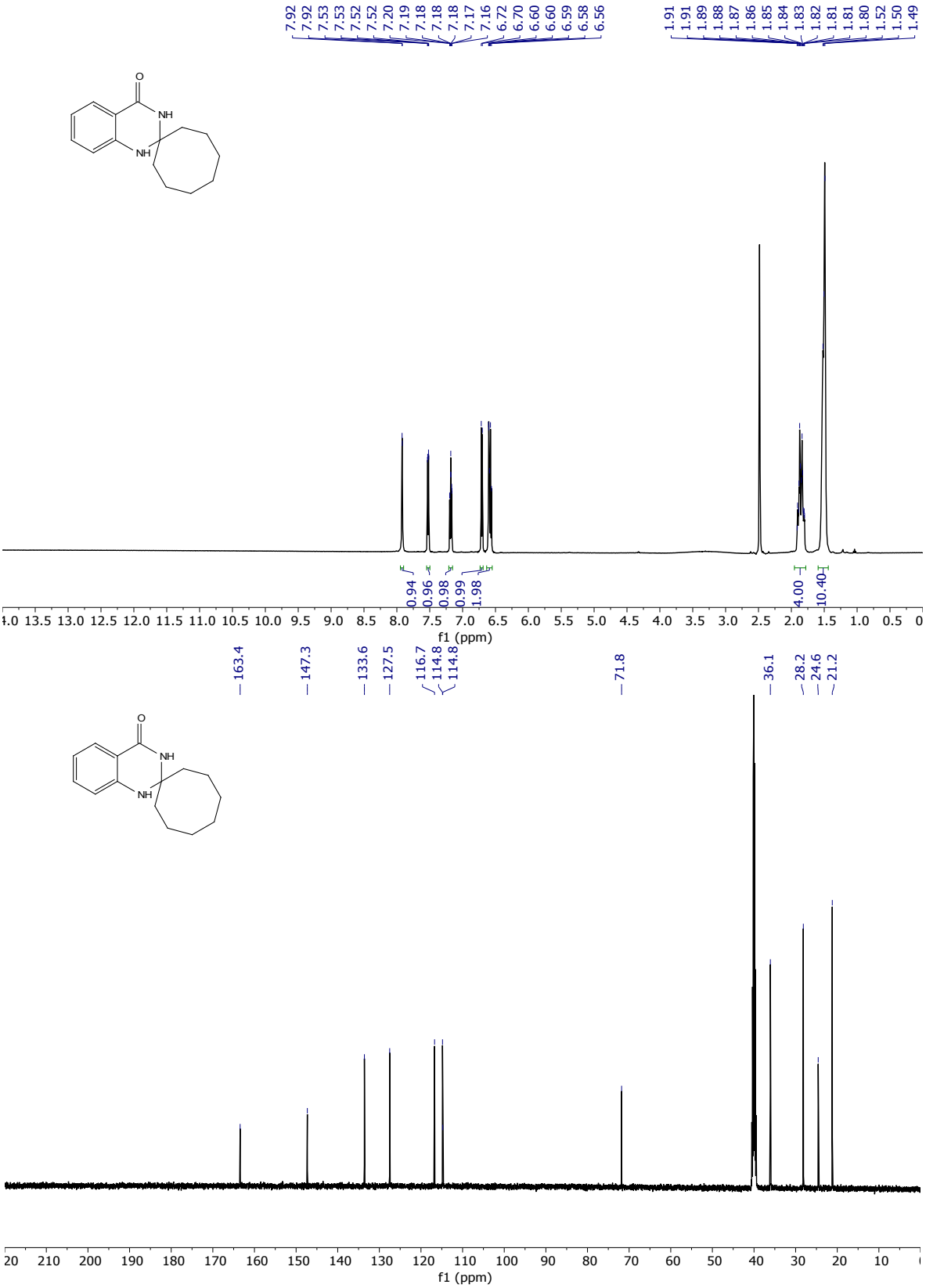

Figure S39. ^{1}H (top) and ^{13}C (bottom) NMR spectra of 1'*H*-spiro[cyclooctane-1,2'-quinazolin]-4'(3'*H*)-one

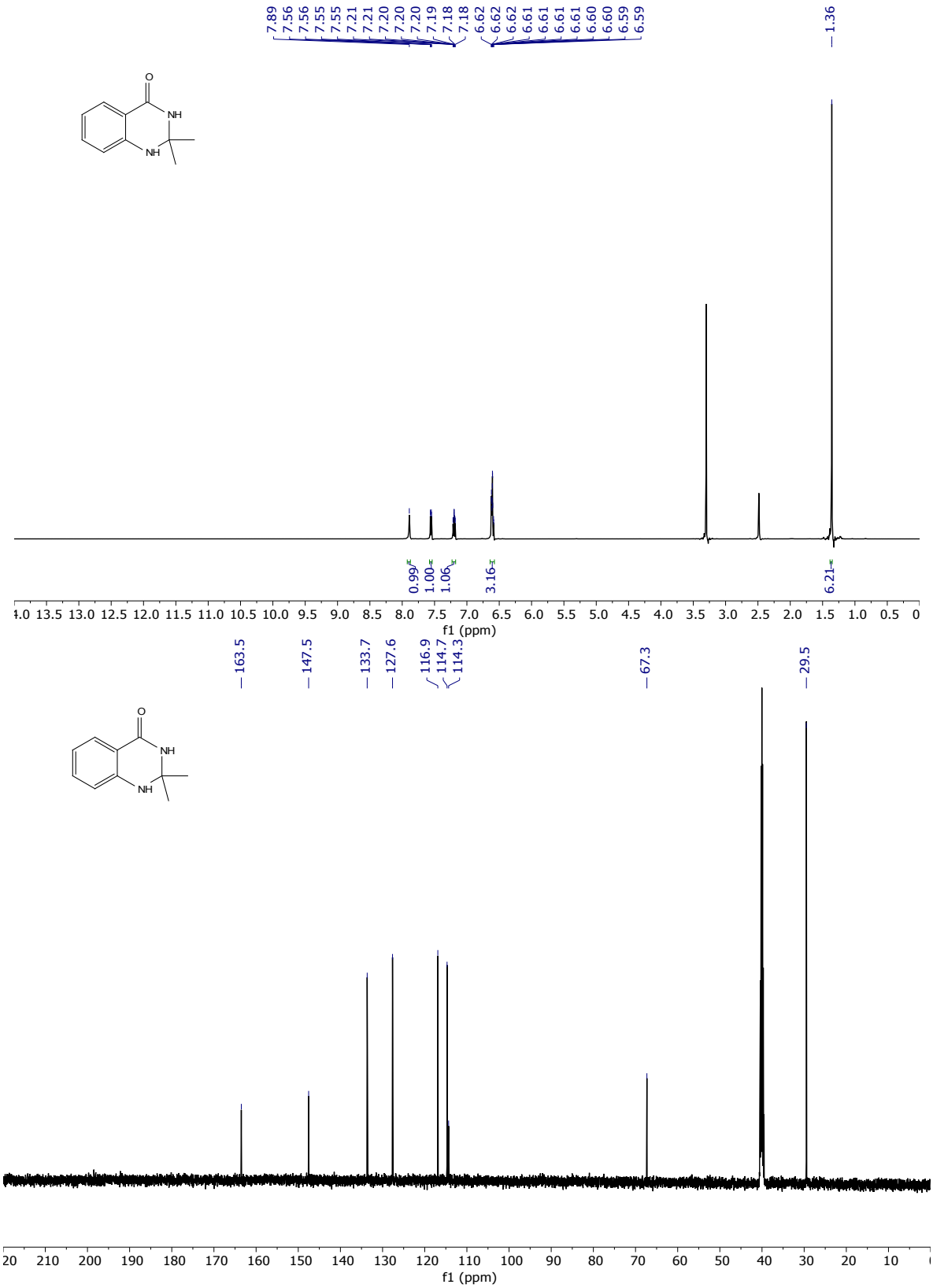

Figure S40. ^{1}H (top) and ^{13}C (bottom) NMR spectra of 2,2-dimethyl-2,3-dihydroquinazolin-4(1*H*)-one

Section 9: References

1 H. Furukawa, N. Ko, Y.B. Go, N. Aratani, S.B. Choi, E. Choi, A.Ö. Yazaydin, R.Q. Snurr, M. O'Keeffe, J. Kim, O.M. Yaghi, *Science*, 2010, 329, 424.

2 H.T.H. Nguyen, L.T.M. Hoang, L.H. Ngo, H.L. Nguyen, C.K. Nguyen, B.T. Nguyen, Q.T. Ton, H.K.D. Nguyen, K.E. Cordova, T. Truong,*Chem. Commun.*, 2013, 51, 17132.

3 S. Ameerunisha, P.S. Zacharias, *J. Chem. Soc., Perkin Trans 2*. 1995, 8, 1679.

4 H.L. Nguyen, T.T. Vu, D.K. Nguyen, C.A. Trickett, T.L.H. Doan, C.S. Diercks, V.Q. Nguyen, K.E. Cordova, *Commun. Chem.,* 2018, 1, 1.

5 T.T.M. Nguyen, H.M. Le, Y. Kawazoe, H.L. Nguyen, *Mater. Chem. Front*., 2018, 2, 2340.

6 D. Feng, K. Wang, Z. Wei, Y.P. Chen, C.M. Simon, R.K. Arvapally, R.L. Martin, M. Bosch, T.F. Liu, S. Fordham, D. Yuan, M.A. Omary, M. Haranczyk, B. Smit, H.C. Zhou, *Nat. Commun.*, 2014, 5, 1.

7 Y. Horiuchi, T. Toyao, K. Miyahara, L. Zakary, D. Do Van, Y. Kamata, T.H. Kim, S.W. Lee, M. Matsuoka, *Chem. Commun*., 2016, 52, 5190.

8 M. Ma, A. Bétard, I. Weber, N.S. Al-Hokbany, R.A. Fischer, N. Metzler-Nolte, *Cryst. Growth Des.,* 2013,13, 2286.

9 A. Fateeva, P. Horcajada, T. Devic, C. Serre, J. Marrot, J.M. Grenèche, M. Morcrette, J.M. Tarascon, G. Maurin, G. Férey, *Eur. J. Inorg. Chem.*2010, 68,3789.

10 P. Horcajada, S. Surblé, C. Serre, D.Y. Hong, Y.K. Seo, J.S. Chang, J.M. Grenèche, I. Margiolaki, G. Férey, *Chem. Commun.*, 2007, 100, 2820.

11 P. Horcajada, F. Salles, S. Wuttke, T. Devic, D. Heurtaux, G. Maurin, A. Vimont, M. Daturi, O. David, E. Magnier, N. Stock, Y. Filinchuk, D. Popov, C. Riekel, G. Férey, C. Serre, *J. Am. Chem. Soc.* 2011,133, 17839.

12 K. R. Reddy, P. Srinivasu, B. D. Raju, M.L. Kantam, K.S. R. Rao, M. Sures, *J. Chem. Sci.*,2014, 126, 527.

13 K.M.L. Taylor-Pashow, J. D. Rocca, Z. Xie, S. Tran, W. Lin, *J. Am. Chem. Soc.* 2009, 131, 14261.

14 M. Dan-Hardi, H. Chevreau, T. Devic, P. Horcajada, G. Maurin, G. Férey, D. Popov, C. Riekel, S. Wuttke, J.C. Lavalley, A. Vimont, T. Boudewijns, D. De Vos, C. Serre, *Chem. Mater.,*2012, 24, 2486.

15 D. Bara, C. Wilson, M. Mörtel, M.M. Khusniyarov, S. Ling, B. Slater, S. Sproules, R.S. Forgan, *J. Am. Chem. Soc.*, 2019, 141, 8346.

16 A. C. McKinlay, J.F. Eubank, S. Wuttke, P.S. Wheatley, P. Bazin, J.C. Lavalley, M. Daturi, A. Vimont, G. De Weireld, P. Horcajada, C. Serre, R.E. Morris, *Chem. Mater*., 2013, 25, 1592.